suggests the importance of $S1PR_2$ signaling in cochlear hair cell survival against ototoxic insults.

References

[1] S. Spiegel, S. Milstien, Sphingosine 1-phosphate: a key cell signaling molecule, J. Biol. Chem. 277 (2002) 25851–25854.
[2] M.J. Kluk, T. Hla, Signaling of sphgosine-1-phosphate via the S1p/EDG-family of G-protein-coupled receptors, Biochim. Biophys. Acta 1582 (2002) 72–80.
[3] S. Spiegel, S. Milstien, Sphingosine 1-phosphate: an enigmatic signaling lipid, Nat. Rev. Mol. Cell Biol. 4 (2003) 397–407.
[4] T. Hla, Signaling and biological actions of sphiogosine 1-phosphate, Pharmacol. Res. 47 (2003) 401–407.
[5] B. Nishimura, K. Tabuchi, M. Nakamagoe, A. Hara, The influences of sphingolipid metabolites on gentamicin-induced hair cell loss of the rat cochlea, Neurosci. Lett. 485 (2010) 1–5.
[6] I. Ishii, J.J. Contos, N. Fukushima, J. Chun, Functional comparisons of the lysophosphatidic acid receptors, LP_{A1}/VZG-1/EDG-2, LP_{A2}/EDG-4, and LP_{A3}/EDG-7 in neural cell lines using a retrovirus expression system, Mol. Pharmacol. 58 (2000) 895–902.
[7] B. Anliker, J. Chun, Cell surface receptors in lysophospholipid signaling, Semin. Cell Dev. Biol. 15 (2004) 457–465.
[8] J.D. Saba, T. Hla, Point-counterpoint sphingosine 1-phosphate metabolism, Circ. Res. 94 (2004) 724–734.
[9] H. Rosen, P.J. Gonzalez-Cabrera, M.G. Sanna, S. Brown, Sphingosine 1-phosphate receptor signaling, Annu. Rev. Biochem. 78 (2009) 743–768.
[10] M. Kono, I.A. Belyantseva, A. Skoura, G.I. Frolenkov, M.F. Starost, J.L. Dreier, D. Lidingtn, S.S. Bloz, T.B. Friedman, T. Hla, R.L. Proia, Deafness and stria vascularis defects in $S1P_2$ receptor-null mice, J. Biol. Chem. 282 (2007) 10690–10696.
[11] D.R. Herr, N. Grillet, M. Schwander, R. Rivera, U. Müller, J. Chun, Sphingosine 1-phosphate (S1P) signaling is required for maintenance of hair cells mainly via activation of $S1P_2$, J. Neurosci. 27 (2007) 1474–1478.
[12] M. Nakamagoe, K. Tabuchi, I. Uemaetomari, B. Nishimura, A. Hara, Estradiol protects the cochlea against gentamicin ototoxicity through inhibition of the JNK pathway, Hear. Res. 261 (2010) 67–74.
[13] A. Forge, Outer hair cell loss and supporting cell expansion following chronic gentamicin treatment, Hear. Res. 19 (1985) 171–182.
[14] A. Forge, L. Li, Apoptotic death of hair cells in mammalian vestibular sensory epithelia, Hear. Res. 139 (2000) 97–115.
[15] K. Tabuchi, K. Pak, E. Chavez, A.F. Ryan, Role of inhibitor of apoptosis protein in gentamicin-induced cochlear hair cell damage, Neuroscience 49 (2007) 213–222.
[16] T. Van de Water, R.J. Ruben, Growth of the inner ear in organ culture, Ann. Otol. Rhinol. Laryngol. 83 (1974) 1–16.
[17] H.M. Sobkowicz, J.M. Loftus, S.M. Slapnick, Tissue culture of the organ of Corti, Acta Otolaryngol. Suppl. 502 (1993) 3–36.
[18] K. Tabuchi, K. Oikawa, T. Hoshino, B. Nishimura, K. Hayashi, E. Yanagawa, T. Warabi, T. Ishii, S. Tanaka, A. Hara, Cochlear protection from acoustic injury by inhibitors of p38 mitogen-activated protein kinase and sequestosome 1 stress protein, Neuroscience 166 (2010) 237–241.
[19] S. Tanaka, K. Tabuchi, T. Hoshino, H. Murashita, S. Tsuji, A. Hara, Protective effects of exogenous GM-1 ganglioside on acoustic injury of the mouse cochlea, Neurosci. Lett. 473 (2010) 237–241.
[20] T. Sanchez, T. Hla, Structural and functional characteristics of S1P receptors, J. Cell. Biochem. 92 (2004) 913–922.
[21] A.J. Maclennan, S.J. Benner, A. Andringe, A.H. Chaves, J.L. Rosing, R. Vesey, A.M. Karpaman, S.A. Cronier, N. Lee, L.C. Erway, M.L. Miller, The $S1P_2$ sphingosine 1-phosphate receptor is essential for auditory and vestibular function, Hear. Res. 220 (2006) 38–48.
[22] L.L. Cunningham, A.G. Cheng, E.W. Rubel, Caspase activation in hair cells of the mouse utricle exposed to neomycin, J. Neurosci. 22 (2002) 8532–8540.

Original Paper

Audiology & Neurotology

Audiol Neurotol 2013;18:335–343
DOI: 10.1159/000354620

Received: March 11, 2013
Accepted after revision: July 22, 2013
Published online: October 2, 2013

Evaluation of the Internal Structure of Normal and Pathological Guinea Pig Cochleae Using Optical Coherence Tomography

Akinobu Kakigi[a] Yuya Takubo[b] Naoya Egami[a] Akinori Kashio[a]
Munetaka Ushio[a] Takashi Sakamoto[a] Shinji Yamashita[b] Tatsuya Yamasoba[a]

[a]Department of Otolaryngology, Faculty of Medicine, and [b]Research Center for Advanced Science and Technology, The University of Tokyo, Tokyo, Japan

Key Words
Cochlea · Optical coherence tomography · Endolymphatic hydrops · Strial atrophy · Organ of Corti

Abstract
Optical coherence tomography (OCT) makes it possible to visualize the internal structures of several organs, such as the eye, in vivo. Although visualization of the internal structures of the inner ear has been used to try and identify certain pathological conditions, attempts have failed mainly due to the thick bony capsule surrounding this end organ. After decalcifying the bony wall of the cochlea with ethylenediamine tetraacetic acid, we could clearly visualize its internal structures by using OCT. We identified endolymphatic hydrops, strial atrophy and damage to the organ of Corti, evident as a distention of Reissner's membrane, thinning of the lateral wall and flattening of the organ of Corti, respectively. When specimens embedded in paraffin, sliced and stained with hematoxylin and eosin (HE) were examined under a light microscope, the OCT images of normal and pathological cochleae were virtually identical with those of the HE specimens, except that the HE specimens exhibited several artifacts unrecognized in OCT images, which were considered to be induced during the preparation process. Since OCT enables one to obtain arbitrary plane images by manipulating the slice axis of the specimens and avoids any misinterpretation due to artifacts induced during histological preparation, our technique would be useful for examining cochlear pathologies without or prior to histological evaluations.
© 2013 S. Karger AG, Basel

Introduction

Structural integrity of the cochlea is required to maintain normal auditory function. Certain types of cochlear pathologies have been known to be closely associated with impaired auditory function. Since the cochlea is housed deeply within the temporal bone, however, it is extremely difficult to examine its structure in vivo. Structural observation has primarily been limited to histological methods, which require several procedures such as chemical fixation, dissection of the tissues, embedment in a mold such as paraffin, and sectioning. These procedures can introduce significant changes in tissue integrity and organization [Slepecky and Ulfendahl, 1988; Brunschwig and Salt, 1997], limiting the generality and overall value of results. To better visualize the internal structure of the cochlea, an emerging noninvasive imaging modality, optical coherence tomography (OCT), has been applied.

KARGER
© 2013 S. Karger AG, Basel
1420–3030/13/0185–0335$38.00/0

E-Mail karger@karger.com
www.karger.com/aud

Akinobu Kakigi
Department of Otolaryngology, Faculty of Medicine, University of Tokyo
7-3-1 Hongo, Bunkyo-ku
Tokyo 113-8655 (Japan)
E-Mail kakigi-tky@umin.ac.jp

Downloaded by Keio University

OCT uses low-coherence interferometry to produce a two-dimensional image of internal tissue microstructures [Huang et al., 1991]. It uses light to discern intrinsic differences in tissue structure and uses coherence gating to localize the origin of the reflected optic signal. Internal tissue microstructures can be visualized with axial and lateral spatial resolutions in the order of 10 μm and a depth of penetration of approximately 2–3 mm depending on tissue translucency. This technology has become widely established for clinical applications in the fields of ophthalmology and dermatology to visualize the translucent tissues of the eye [Izatt et al., 1994] and superficial tissues of the skin [Welzel, 2001].

Clinical use of OCT has since been extended to the fields of cardiology and gastroenterology in visualizing deeper structures such as coronary vessels [Jang et al., 2002] and the gastrointestinal tract [Shen and Zuccaro, 2004]. Most recently, OCT has been used in the field of otolaryngology to visualize the larynx [Wong et al., 2005]. However, clinical use of OCT has been limited in other organs including the inner ear because of its relatively limited depth of penetration and the turbidity of most biological tissues. In fact, previous studies allowed visualization of only limited areas of the cochleae [Wong et al., 2004; Lin et al., 2008; Sepehr et al., 2008; Subhash et al., 2010]. For example, Sepehr et al. [2008] drilled the otic capsule of pigs obtained within 1 h of sacrifice and found that in the areas of thinned bone, acceptable images were obtained of the spiral ligament, stria vascularis, Reissner's membrane, basilar membrane, tectorial membrane, scala media, scala tympani and scala vestibuli; however, the bone was too thick for adequate light penetration in the areas where it was not thinned.

Subhash et al. [2010] obtained in vivo OCT images of a portion of the apical, middle and basal turns of the mouse cochlea through a surgically prepared opening via the bone of the bulla. They demonstrated that spectral-domain OCT could be used for in vivo imaging of important morphological features within the mouse cochlea, such as the otic capsule and structures within, including Reissner's membrane, the basilar membrane, the tectorial membrane, the organ of Corti and the modiolus of the apical and middle turns, but the resolution and quality were unsatisfactory.

In the current study, we observed the cochleae by OCT after decalcification of the otic bony capsule. We could clearly visualize normal internal structures of the cochleae and identify endolymphatic hydrops (EH), strial atrophy and damage to the organ of Corti, which appeared as a distention of Reissner's membrane, thinning of the lateral wall and flattening of the organ of Corti, respectively. This technology can prevent the misinterpretation of histological findings due to artifacts induced during histological preparation and thus is of great value in investigating the internal structural change of various types of cochlear damage.

Materials and Methods

Animals

A total of 20 Hartley guinea pigs with a positive Preyer reflex and weighing approximately 300 g were used. They were allocated to the following four groups, each consisting of 5 animals: (1) normal control group (no surgical procedure or treatment); (2) EH group (electrocauterization of the endolymphatic sac (ES), and a 4-week feeding); (3) kanamycin sulfate-ethacrynic acid (KM-EA) group (no surgical procedures, but intravenous administration of KM and EA and a 2-day feeding); and (4) streptomycin sulfate (SM) group (perilymphatic perfusion with 20% SM and a 4-month feeding). These experiments were approved by the Tokyo University animal care and use committee, and conformed to the Animal Welfare Act and the guiding principles for animal care produced by the Ministry of Education, Culture, Sports and Technology, Japan.

Surgical Procedure for the Electrocauterization of ES

EH can be either primary or secondary. Primary idiopathic EH (known as Ménière's disease) occurs for no known reason, while secondary EH appears to occur in response to an event or underlying condition (e.g. following head trauma or ear surgery, or with other inner ear disorders, allergies or systemic disorders such autoimmune disorders). EH was initially reported in patients with Ménière's disease independently by Yamakawa [1938] and Hallpike and Cairns [1938] and has since been found to be frequent in patients with Ménière's disease. EH represents a histopathological finding in which the structures bounding the endolymphatic space are distended by an enlargement of endolymphatic volume. The most widely studied animal model of EH was created by surgical ablation of the endolymphatic duct and sac in guinea pigs [Kimura and Schuknecht, 1965; Kimura, 1967].

To induce EH, we performed electrocauterization of the ES. Animals were anesthetized with an intraperitoneal injection of ketamine (35 mg/kg) and xylazine (5 mg/kg) and received local anesthesia with Xylocaine in sterile conditions. Then, they were placed in a prone position with a head holder and underwent a dorsal midline scalp incision under a Carl Zeiss operation microscope. The left occipital bone was removed to visually expose the ES via an epidural occipital approach. Then, the extraosseous portion of the sac was cauterized electrically so as not to injure the sigmoid sinus with the bipolar electrocoagulator (Surgitron Model FFPF; Ellman International Inc., Hewlett, N.Y., USA). The skin incision was sutured and the animals were allowed to survive for 4 weeks.

Procedures for Intravenous Administration of KM and EA

Auditory hair cells can be damaged and lost as a consequence of acoustic trauma, treatment with ototoxic agents, infections, autoimmune pathologies and genetic susceptibilities or as a part of the aging process. The loss of auditory hair cells in the human cochlea is a leading cause of permanent hearing deficits, currently affecting an estimated 600 million worldwide. In recent studies, loop diuret-

Downloaded by:
Keio University
131.113.126.67 - 3/14/2014 5:50:36 AM

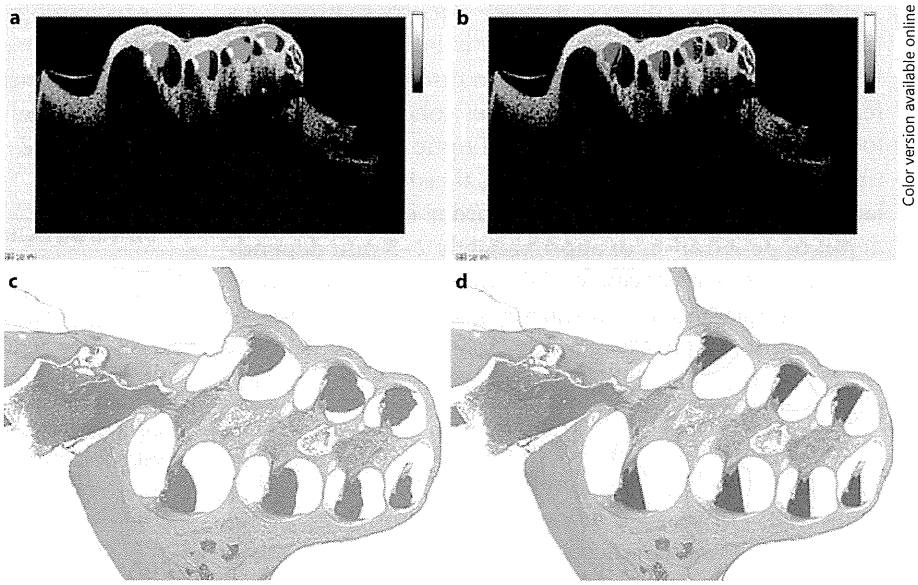

Fig. 1. Parameters for quantitative assessment of changes in endolymphatic space, organ of Corti and lateral wall. **a** Cross-sectional area of the dilated scala media (red areas), organ of Corti (yellow areas) and upper part of the lateral wall over the extended line of the lower level of the basilar membrane (green area) in an OCT image. **b** Cross-sectional area of the original scala media (blue areas) enclosed by a straight line segment. This line segment represents the position of the idealized Reissner's membrane at the upper margin of the stria vascularis to its normal medial attachment at the spiral limbus. **c** Cross-sectional area of the dilated scala media (red areas) of an HE specimen. **d** Cross-sectional area of the original scala media (blue areas) of an HE specimen. Colors refer to the online version only.

ics have been used to augment the ototoxic effect of aminoglycoside antibiotics and eliminate hair cells in mammals [Xu et al., 1993; Yamasoba and Kondo, 2006; Kashio et al., 2007; Taylor et al., 2008].

To induce degeneration of the organ of Corti, animals were given KM (Meiji, Tokyo, Japan) and EA (Sigma-Aldrich). They were anesthetized with an intraperitoneal injection of ketamine (35 mg/kg) and xylazine (5 mg/kg). A single dose of KM (400 mg/kg) was injected subcutaneously; 2 h after the KM injection, EA (50 mg/kg) was infused into the jugular vein as previously described [Yamasoba and Kondo, 2006]. The animals were then allowed to survive for 2 days after deafening.

Procedures for Perilymphatic Perfusion with 20% SM

Strial atrophy is one of the leading causes of deafness and three major etiologic factors have been reported: hereditary strial hypoplasia/atrophy [Gates et al., 1999; Ohlemiller et al., 2006], aging [Schuknecht and Gacek, 1993] and ototoxicity due to loop diuretics or the erythromycin group of antibiotics [Arnold et al., 1981; McGhan and Merchant, 2003].

To induce both hair cell loss and strial atrophy, animals underwent perilymphatic perfusion with 20% SM (Meiji) dissolved in Ringer's solution (Fuso, Osaka, Japan). The animals were anesthetized with an intraperitoneal injection of ketamine (35 mg/kg) and xylazine (5 mg/kg). The left cochlea was exposed using the lateral approach, and both the scala tympani and the scala vestibuli of four cochlear turns were perfused as follows. A 20% SM solution was gently perfused into the scala tympani through the round window membrane until the solution flowed out from the drilled hole adjacent to the oval window, as previously described [Terayama et al., 1977]. After the perfusion, the tympanic cavity was cleaned, the skin incision closed and the animals allowed to survive for 4 weeks.

OCT and Histological Observations

To observe the cochleae by OCT, all animals were given physiological saline from the left ventricle under deep anesthesia with ketamine and xylazine and fixed with 10% formalin. Both temporal bones were obtained immediately following the fixation and kept in a 10% formalin solution for 1 week. Subsequently, the specimens underwent decalcification in ethylenediamine tetraacetic acid (EDTA) for 14 days. Then we obtained midmodiolar images of the cochleae by using the Santec OCT system controlled by Inner Vision (Santec Co., Aichi, Japan). The characteristics of the Santec OCT system were as follows. The center wavelength band was 1,320 nm and the band width 90 nm. The axial and lateral resolutions were 12.0 and 17.0 μm, respectively. The measurement speed and frame rate were 50,000 lines/scan and 100 frames/s, respectively. The image depth and width were 6.0 and 10.0 mm, respectively. After OCT images were obtained, the temporal bones were dehydrated in increasingly higher concentrations of alcohol, embedded in paraffin and cut serially at 6 μm in the plane parallel to the modiolus to obtain approximately the same plane as the OCT image. The sections were stained with hematoxylin and eosin (HE) and observed under a light microscope [light microscopic mode of the BZ-9000 fluorescence microscope (Keyence, Osaka, Japan) controlled by BZ-II Analyzer (Keyence) software].

Quantitative Assessment of Endolymphatic Space, Organ of Corti and Lateral Wall

We used the digital image measurement software Micro Analyzer version 1.1 (Nippon Poladigital Co. Ltd, Tokyo, Japan) for quantitative assessment. In the EH group, we compared the degree of EH between OCT and HE images. For the quantitative assessment of endolymphatic space variations of the cochlea, we measured the increase in the cross-sectional area of the scala media (IR-S) over that in the midmodiolar sections. For this analysis, we used the following two parameters in the basal, second, third and apical turns, not including the hook portion: (1) the cross-sectional area of the dilated scala media (fig. 1a, c; red areas) and (2) the cross-sectional area of the original scala media (fig. 1b, d; blue areas) which were enclosed by a straight line segment. This line segment represents the position of the idealized Reissner's membrane at the upper margin

Downloaded by Keio University

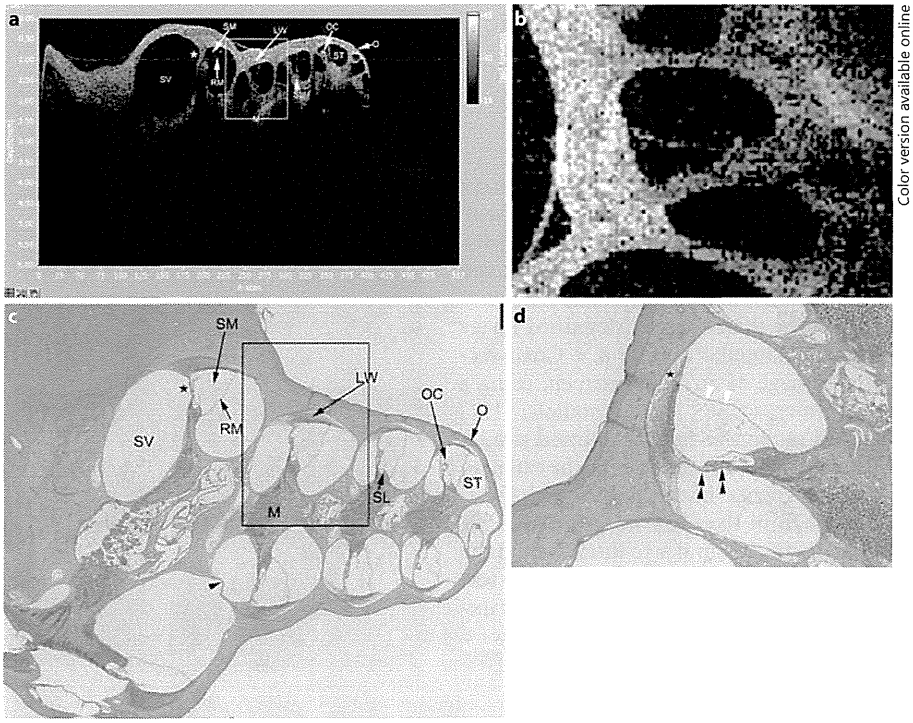

Color version available online

Fig. 2. a Representative cross-sectional OCT image of all turns of the spiral-shaped cochlea. **b** Magnified image (turned 90°) of the rectangular area in **a**. **c** Cross-sectional image of an HE specimen, using a light microscope. HE specimens exhibited several artifacts such as bending of the interscalar septum and basilar membrane and folding of Reissner's membrane as a consequence of separating the spiral ligament from the bony wall. The proportion of the area of the organ of Corti is smaller in the HE specimen (star) than in the OCT image (**a**; white star), especially in the basal turn. **d** Magnified image of the rectangular area in **c**. O = Otic capsule; M = modiolus; RM = Reissner's membrane; OC = organ of Corti; SL = spiral limbus; LW = lateral wall consisting of stria vascularis and spiral ligament; ST = scala tympani; SM = scala media; SV = scala vestibuli; arrowhead = bending of interscalar septum; double arrowheads = bending of basilar membrane; white arrowheads = folding of Reissner's membrane; asterisk = separating spiral ligament from bony wall.

of the stria vascularis to its normal medial attachment at the spiral limbus. From these parameters, we calculated the increase (%) in IR-S in the four turns with the following formula:

Total IR-S (%) = 100 × (red area – blue area)/blue area

Statistical Analysis

Data are presented as means ± SD, and they were compared by the paired Student t test. Differences were regarded as significant when $p < 0.05$.

We compared the degree of flattening of the organ of Corti and strial atrophy between the normal control and KM-EA groups and between the normal control and SM groups, respectively. To analyze the flattening of the organ of Corti, we used the following parameter in the basal, second, third and apical turns, not including the hook portion: the cross-sectional area of the organ of Corti (fig. 1a; yellow areas). Data for each turn were separately compared by Student's t test, and a difference was regarded as significant when $p < 0.05$. For the analysis of strial atrophy, we used the following parameter in the second turn: the cross-sectional area of the upper part of the lateral wall over the extended line of the lower level of the basilar membrane (fig. 1a; green area). We selected the second turn for the assessment because there was no proliferative change such as fibrosis.

Results

Normal Control Group

OCT provided detailed internal structures of the normal cochleae. We clearly identified not only the otic capsule and the modiolus, but also Reissner's membrane, the organ of Corti, the spiral limbus, the lateral wall consisting of the stria vascularis and spiral ligament in all four turns of the midmodiolar section (fig. 2a, b). The scalae tympani, media and vestibuli were clearly distinguishable. The OCT images were virtually identical with the corresponding histological sections (fig. 2c, d), although the HE specimens exhibited several artifacts such as the bending of the interscalar septum and basilar membrane and the folding of Reissner's membrane as a consequence of the separation of the spiral ligament from the bony wall. Concerning the organ of Corti, the proportion of the area was smaller in the HE specimen than in the OCT image, especially in the basal turn.

EH Group

OCT clearly demonstrated the presence of EH in all 5 cases 4 weeks after electrocauterization of the ES. In a case shown in figure 3a, mild but distinct hydrops was observed in the basal and second turns, and the hydrops was most evident in the third turn (fig. 3b, d). The spiral ligament, stria vascularis and organ of Corti appeared normal. A midmodiolar HE-stained section in this ear showed similar histological findings (fig. 3c), although the extent of EH was greater in the histological specimens

Downloaded by
Keio University
133.1.113.100 - 3/14/2014 4:50:35 AM

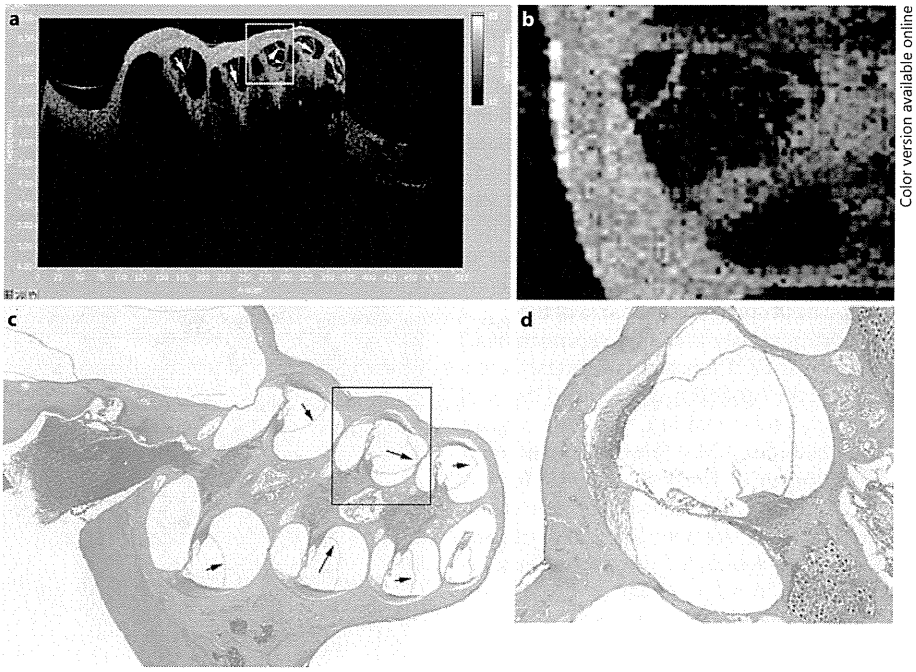

Color version available online

Fig. 3. **a** Representative cross-sectional OCT image of the cochlea in animals with electrocauterization of the ES. Mild but distinct hydrops was found in the basal and second turns, and hydrops was most evident in the third turn. **b** Magnified image of the rectangular area in **a**. **c** Cross-sectional image of an HE specimen, using a light microscope. A midmodiolar HE-stained section in this ear showed similar histological findings, although the extent of EH was greater in the histological specimens than in the OCT images. There are several artifacts similar to those seen in the normal cochlea. Note that hydrops was most evident in this turn. **d** Magnified image of the rectangular area in **c**. Arrows = Distention of Reissner's membrane.

than in the OCT images (fig. 4). Further, there were several artifacts similar to those seen in the normal cochlea. Figure 4 shows the IR-S in OCT and HE images: 54.3 ± 4.05% and 62.4 ± 6.51%, respectively. The IR-S was statistically larger in the HE than in the OCT images (paired Student's t test, $p < 0.05$).

KM-EA Group

Two days after the treatment with KM and EA, all animals lost the Preyer reflex and exhibited degeneration of the organ of Corti in all turns (fig. 5a). In a case shown in figure 5b, the flattening of the organ of Corti was obvious in the third and apical turns, whereas the spiral ligament and stria vascularis appeared normal. A slight collapse of Reissner's membrane was seen in all four turns. A midmodiolar HE-stained section in this ear showed similar histological findings, except that there was no collapse of Reissner's membrane (fig. 5e, f). The difference regarding Reissner's membrane between the OCT and histological findings may have been caused by histological preparation. Further, there were several artifacts similar to those seen in the normal cochlea. To assess the effects of KM-EA treatment on the organ of Corti, a comparison of the normalized size ratio of the organ of Corti (size of the targeted organ of Corti/average of the size of the normal organ of Corti) was made between the normal control and KM-EK groups, using OCT images. The normalized size

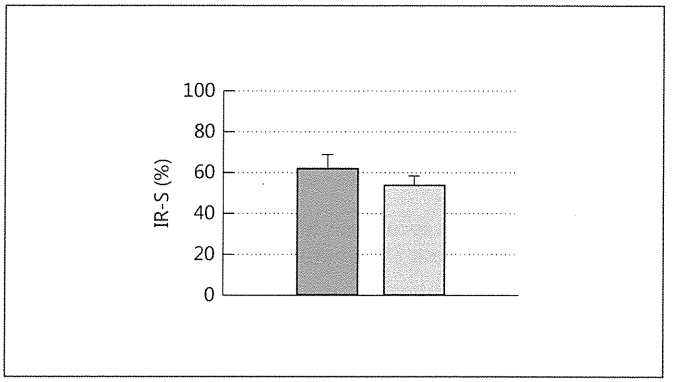

Fig. 4. Comparison of IR-S between OCT (light gray) and HE (dark gray) images. The IR-S (means ± SD) on the OCT and HE images were 54.3 ± 4.05% (n = 5) and 62.4 ± 6.51% (n = 5), respectively. The IR-S on the HE images was statistically larger than that on the OCT images (paired Student's t test, $p < 0.05$).

ratios of the basal, second, third and apical turns were 0.63 ± 0.14, 0.78 ± 0.16, 0.51 ± 0.10 and 0.58 ± 0.14, respectively, in the KM-EA group (n = 5; fig. 6). The KM-EA treatment resulted in a marked decrease in normalized size ratio of the organ of Corti. The decreases in the basal, second, third and apical turns were significant at $p < 0.001$, $p < 0.05$, $p < 0.001$ and $p < 0.05$, respectively (Student's t test).

Downloaded by Mayo University

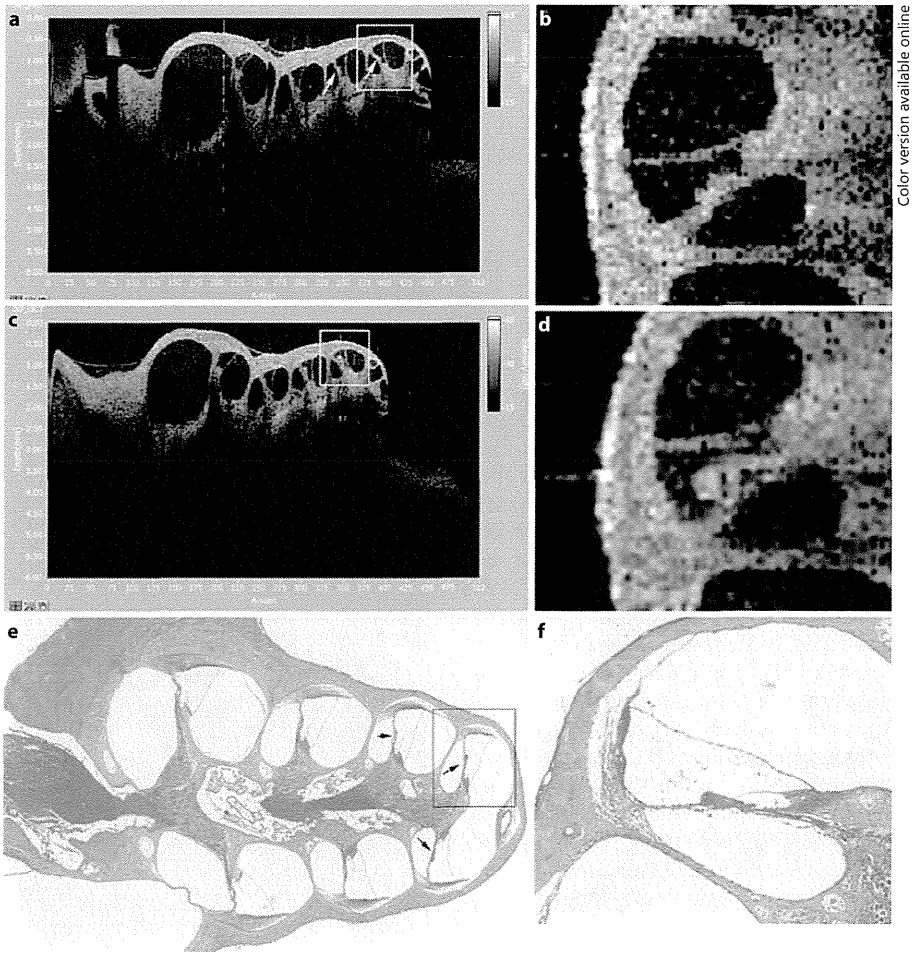

Color version available online

Fig. 5. a Representative cross-sectional OCT image of the cochlea in animals with intravenous administration of KM and EA. The flattening of the organ of Corti was obvious in the third and apical turns. The spiral ligament and stria vascularis appeared normal. A slight collapse of Reissner's membrane was seen in all four turns. **b** Magnified image of the rectangular area in **a**. **c** Representative cross-sectional OCT image of the cochlea in the normal group. **d** Magnified image of the rectangular area in **c**. **e** A midmodiolar HE-stained section showed similar histological findings, although there was no collapse of Reissner's membrane. There are several artifacts similar to those seen in the normal cochlea. Note that flattening of the organ of Corti was evident. **f** Magnified image of the rectangular area in **e**. Arrows = Flattening of the organ of Corti.

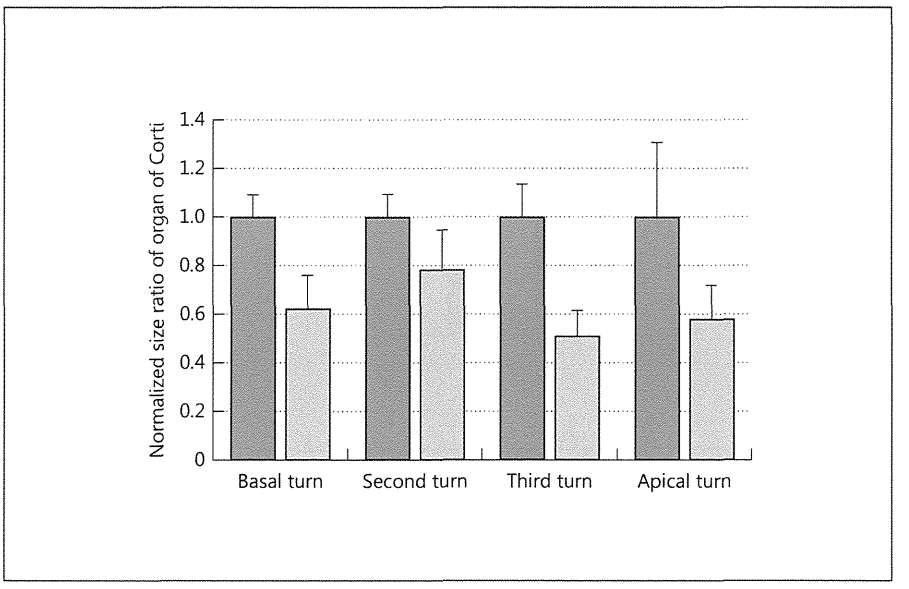

Fig. 6. Comparison of normalized size ratio (size of organ of Corti/averaged size of normal organ of Corti) of organ of Corti between normal control (dark gray) and KM-EA (light gray) groups, using OCT images. The normalized size ratios (means ± SD) of the basal, second, third and apical turns were 1.00 ± 0.09, 1.00 ± 0.09, 1.00 ± 0.14 and 1.00 ± 0.31, respectively, in the normal control group (n = 5), and 0.63 ± 0.14, 0.78 ± 0.16, 0.51 ± 0.10 and 0.58 ± 0.14, respectively, in the KM-EA group (n = 5). The decreases in the basal, second, third and apical turns were significant at $p < 0.001$, $p < 0.05$, $p < 0.001$ and $p < 0.05$, respectively (Student's t test).

Downloaded by
Keio University
133.113.160.67 - 3/11/2013 5:50:35 AM

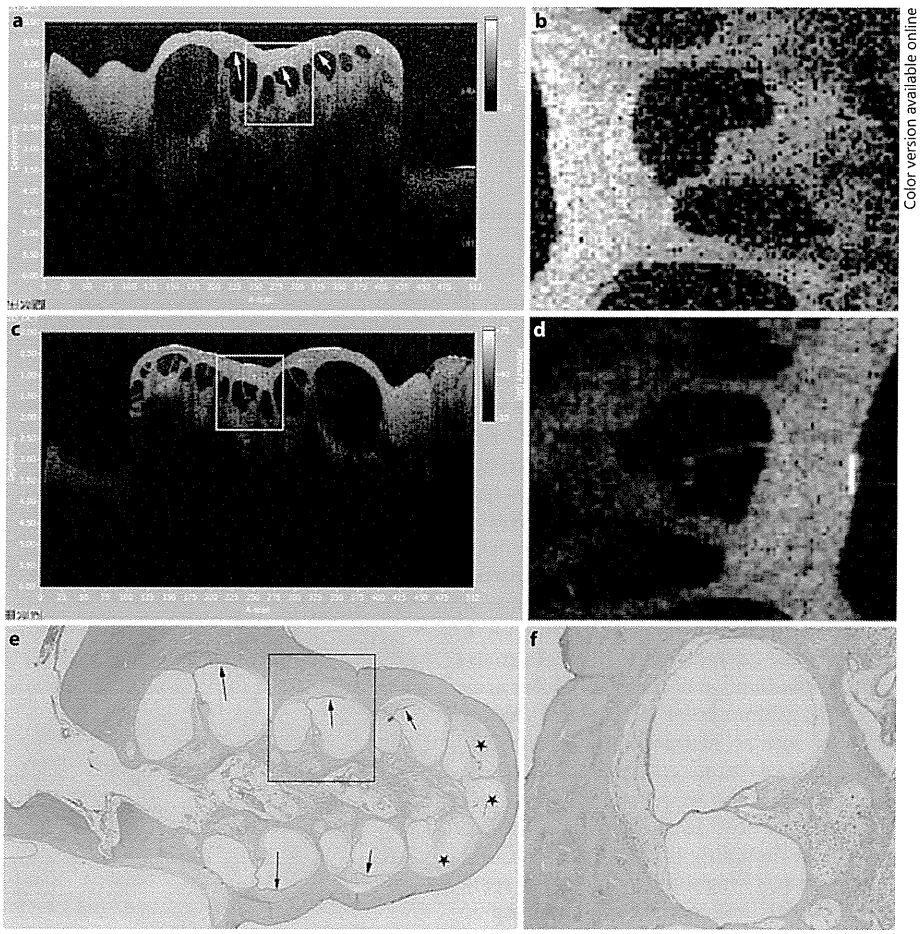

Color version available online

Fig. 7. **a** Representative cross-sectional OCT image of the cochlea in animals with perilymphatic perfusion with SM. Strial atrophy and flattening of the organ of Corti were seen in the basal, second and third turns. The strial atrophy reflected that the curvature of the medial surface increased in the lateral wall. A remarkable collapse of Reissner's membrane was also seen. In the apical turn, the fibrosis of the organ was remarkable. **b** Magnified image of the rectangular area in **a**. **c** Representative cross-sectional OCT image of the cochlea in the control ear. **d** Magnified image of the rectangular area in **c**. **e** Optical cross-sectional image of an HE specimen, using a light microscope. There are the same artifacts in the HE specimen as seen in the normal cochlea. **f** Magnified image of the rectangular area in **e**. Arrows = Strial atrophy; stars = fibrosis.

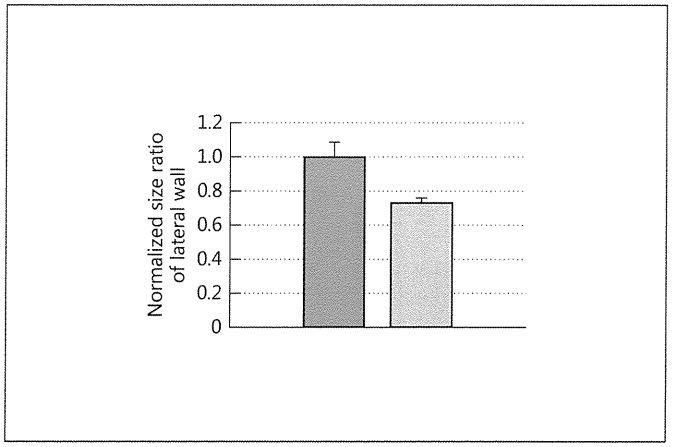

Fig. 8. Comparison of normalized size ratio (size of lateral wall/averaged size of normal lateral wall) of lateral wall between normal control (dark gray) and SM (light gray) groups, using OCT images. The normalized size ratio (mean ± SD) of the second turn was 1.00 ± 0.08 in the normal control group (n = 5) and 0.74 ± 0.02 in the SM group (n = 5). The decrease in the second turn was significant at $p < 0.001$ (Student's t test).

SM Group

The strial atrophy and damage to the organ of Corti were evident in all cases 4 weeks after perilymphatic perfusion with 20% SM (fig. 7a, b). Strial atrophy and flattening of the organ of Corti were seen mostly in the basal, second and third turns. The strial atrophy reflected that the curvature of the medial surface increased in the lateral wall. The remarkable collapse of Reissner's membrane was also seen mostly in the basal, second and third turns. In some animals, fibrosis was observed in the apical part of the cochlea. The OCT images were comparable with the corresponding histological sections (fig. 7e, f), although the loss of spiral ganglion cells observed in the HE specimen could not be visualized by OCT because of the limited spatial resolution and depth of penetration. To assess the effects of SM treatment on the lateral wall, a comparison of the normalized size ratio of the lateral wall was made between the normal control and SM groups, using OCT images. The normalized size ratio of the second turn was 0.74 ± 0.02 in the SM group (n = 5;

Downloaded by Keio University

fig. 8). SM treatment resulted in a marked decrease in the normalized size ratio of the lateral wall. The decrease in the second turn was significant at $p < 0.001$ (Student's t test).

Discussion

The current study demonstrated that by decalcifying the bony wall of the cochlea with EDTA, the internal structures of the cochlea could be clearly visualized by OCT. The OCT images of the normal cochleae were significantly improved compared with those from previous reports [Wong et al., 2004; Lin et al., 2008; Sepehr et al., 2008; Subhash et al., 2010]. We found that OCT could prevent unnecessary misinterpretations due to artifacts introduced during the preparation of specimens for conventional histological examination. We could also demonstrate that three major cochlear pathologies, i.e. EH, hair cell degeneration and strial atrophy, could be clearly visualized by using OCT.

EH is commonly observed in patients with Ménière's disease and may also occur following head trauma or ear surgery, or in other inner ear disorders, allergies or systemic disorders such autoimmune disorders. The pathophysiology of Ménière's disease has been studied using animal models, and surgical ablation of the endolymphatic duct and sac of guinea pigs [Kimura and Schuknecht, 1965; Kimura, 1967] has most widely been used. It is impossible to determine the presence of EH by using physiological tests such as the auditory brainstem response or caloric test, since such examinations provide only information on the extent of damage to hearing or vestibular function. Thus, it is mandatory to evaluate the presence/absence and extent of EH by histological examination in animals. Schuknecht [1987, 1993] established a standard procedure for the morphological study of the human temporal bone that involved formalin fixation, EDTA decalcification, celloidin embedding and serial sectioning. Celloidin and paraffin are the two common embedding media used for histopathologic study of the human temporal bone by light microscopy. Although celloidin embedding permits excellent morphologic assessment, celloidin is difficult to remove, and there are significant restrictions on success with immunostaining. Other potential disadvantages of the use of celloidin include the length of time needed for embedment. Embedding in paraffin allows immunostaining to be performed, but the preservation of cellular detail within the membranous labyrinth is relatively poor [Merchant et al., 2006]. During the preparation process, the specimen must be embedded in a mold such as paraffin or celloidin, and such a process, especially with paraffin, is known to induce significant artifacts, making it difficult to evaluate the extent of EH. Compared with the OCT images in our study, paraffin-embedded HE specimens exhibited EH to a greater extent and also showed artifacts such as bending of the interscalar septum and basilar membrane and folding of Reissner's membrane. These findings suggest that estimating the extent of EH and associated tissue damage can be done more precisely using OCT images than by histological evaluation, especially using paraffin-embedded HE specimens. Further, the specimen can be easily used for molecular and immunohistochemical techniques after OCT imaging.

We also observed that OCT could visualize the degeneration of the organ of Corti, collapse of Reissner's membrane and strial atrophy 2 days after systemic administration of a combination of KM and EA and 4 weeks after perfusion with 20% SM throughout the cochlea. An intravenous administration of KM and EA induces hair cell degeneration and scar formation, which start 3 h after drug administration [Raphael and Altschuler, 1991]. In Raphael and Altschuler's report, mild flattening of the organ of Corti was seen from 9 h after drug administration. At this time, the outer hair cells from all three rows are replaced by supporting cells, which fill the entire space between the tunnel of Corti and Hensen cells. However, the inner hair cells are present and the shape of the organ of Corti is preserved. In our study, OCT could detect such degeneration as a reduction in the size of the organ of Corti, which could not be observed in the basal turn of an HE-stained section because of the artifacts produced (fig. 2a, b). Further, OCT could detect a mild collapse of Reissner's membrane, which again could not be detected in HE-stained sections. These findings suggest that estimating the extent of the degeneration of the organ of Corti and associated tissue damage (e.g. collapse of Reissner's membrane) can be done more precisely by using OCT images than histological evaluation, especially with paraffin-embedded HE specimens. Conversely, although OCT could detect severe degeneration of the organ of Corti, strial atrophy and remarkable collapse of Reissner's membrane in the SM group, it could not detect the loss of spiral ganglion cells, which could be observed in the HE specimens.

The method shown here cannot be applied to clinical evaluations of pathology in the cochlea. Therefore, we still need other novel technologies to improve the transparency and translucency of OCT.

Downloaded by
Keio University
131.113.150.67 - 3/11/2014 3:58:36 AM

Conclusions

By decalcifying the bony wall of the cochlea, we could clearly and widely visualize the internal structures of normal and pathological cochleae. We could easily manipulate the slice axis to obtain arbitrary plane views using OCT, and we could demonstrate EH, strial atrophy and damage to the organ of Corti as a distention of Reissner's membrane, a thinning of the lateral wall and a flattening of the organ of Corti, respectively. The OCT images of normal and pathological cochleae were virtually identical with those of HE specimens, except that the extent of EH was overestimated in histological images compared with OCT images and that there were several artifacts in the HE specimen, such as bending of the interscalar septum and basilar membrane, folding of Reissner's membrane, separation of the spiral ligament from the bony wall, and flattening of the organ of Corti in the basal turn, which were not seen in the OCT images. These findings indicate that observing the decalcified cochlea by using OCT would be of great value when examining cochlear pathology, especially EH, prior to or without histological examinations.

Disclosure Statement

This study was supported by a Health and Labor Science Research Grant for Research on Specific Diseases (Vestibular Disorders) from the Ministry of Health, Labor and Welfare of Japan, and by grants from the Ministry of Education, Science, Culture and Sports, Japan (No. 21592159) and by the Funding Program for Next Generation World-Leading Researchers (NEXT Program) of the Japan Society for the Promotion of Science (JSPS). We have no conflicts of financial interest in this paper.

References

Arnold W, Nadol JB Jr, Weidauer H: Ultrastructural histopathology in a case of human ototoxicity due to loop diuretics. Acta Otolaryngol 1981;91:399–414.

Brunschwig AS, Salt AN: Fixation-induced shrinkage of Reissner's membrane and its potential influence on the assessment of endolymph volume. Hear Res 1997;114:62–68.

Gates GA, Couropmitree NN, Myers RH: Genetic associations in age-related hearing thresholds. Arch Otolaryngol Head Neck Surg 1999; 125:654–659.

Hallpike CS, Cairns HWB: Observations of the pathology of Ménière's syndrome. Proc R Soc Med 1938;31:1317–1336.

Huang D, Swanson EA, Lin CP, Schuman JS, Stinson WG, Chang W, Hee MR, Flotte T, Gregory K, Puliafito CA, Fujimoto JG: Optical coherence tomography. Science 1991;254:1178–1181.

Izatt JA, Hee MR, Swanson EA, Lin CP, Huang D, Schuman JS, Puliafito CA, Fujimoto JG: Micrometer-scale resolution imaging of the anterior eye in vivo with optical coherence tomography. Arch Ophthalmol 1994;112:1584–1589.

Jang IK, Bouma BE, Kang DH, Park SJ, Park SW, Seung KB, Cho, KB, Shishkov M, Schlendorf K, Pomerantsev E, Houser SL, Aretz HT, Tearney GJ: Visualization of coronary atherosclerotic plaques in patients using optical coherence tomography: comparison with intravascular ultrasound. J Am Coll Cardiol 2002;39:604–609.

Kashio A, Sakamoto T, Suzukawa K, Asoh S, Ohta S, Yamasoba T: A protein derived from the fusion of TAT peptide and FNK, a Bcl-x_L derivative, prevents cochlear hair cell death from aminoglycoside ototoxicity in vivo. J Neurosci Res 2007;85:1403–1412.

Kimura RS: Experimental blockage of the endolymphatic duct and sac and its effect on the inner ear of the guinea pig. Ann Otol Rhinol Laryngol 1967;76:664–687.

Kimura RS, Schuknecht HF: Membranous hydrops in the inner ear of the guinea pig after obliteration of the endolymphatic sac. Pract Otorhinolaryngol (Basel) 1965;27:343–354.

Lin J, Staecker H, Jafri MS: Optical coherence tomography imaging of the inner ear: a feasibility study with implications for cochlear implantation. Ann Otol Rhinol Laryngol 2008; 117:341–346.

McGhan LJ, Merchant SN: Erythromycin ototoxicity. Otol Neurotol 2003;24:701–702.

Merchant SN, Burgess B, O'Malley J, Jones D, Adams JC: Polyester wax: a new embedding medium for the histopathologic study of human temporal bones. Laryngoscope 2006;116: 245–249.

Ohlemiller KK, Lett JM, Gagnon PM: Cellular correlates of age-related endocochlear potential reduction in a mouse model. Hear Res 2006;220:10–26.

Raphael Y, Altschuler RA: Scar formation after drug-induced cochlear insult. Hear Res 1991; 51:173–184.

Schuknecht H: Temporal bone collections in Europe and the United States: observations on a productive laboratory, pathologic findings of clinical relevance, and recommendations. Ann Otol Rhinol Laryngol 1987;130:1–19.

Schuknecht H: Methods of removal, preparation and study; in Schuknecht H (ed): Pathology of the Ear, ed 2. Philadelphia, Lea & Febiger, 1993, pp 1–29.

Schuknecht HF, Gacek MR: Cochlear pathology in presbycusis. Ann Otol Rhinol Laryngol 1993;102:1–16.

Sepehr A, Djalilian HR, Chang JE, Chen Z, Wong BJ: Optical coherence tomography of the cochlea in the porcine model. Laryngoscope 2008;118:1449–1451.

Shen B, Zuccaro G Jr: Optical coherence tomography in the gastrointestinal tract. Gastrointest Endosc Clin N Am 2004;14:555–571, x.

Slepecky N, Ulfendahl M: Glutaraldehyde induces cell shape changes in isolated outer hair cells from the inner ear. J Submicrosc Cytol Pathol 1988;20:37–45.

Subhash HM, Davila V, Sun H, Nguyen-Huynh AT, Nuttall AL, Wang RK: Volumetric in vivo imaging of intracochlear microstructures in mice by high-speed spectral domain optical coherence tomography. J Biomed Opt 2010; 15:036024.

Taylor RR, Nevill G, Forge A: Rapid hair cell loss: a mouse model for cochlear lesions. J Assoc Res Otolaryngol 2008;9:44–64.

Terayama Y, Kaneko Y, Kawamoto K, Sakai N: Ultrastructural changes of the nerve elements following disruption of the organ of Corti. I. Nerve elements in the organ of Corti. Acta Otolaryngol 1977;83:291–302.

Welzel J: Optical coherence tomography in dermatology. Skin Res Technol 2001;7:1–9.

Wong BJ, Jackson RP, Guo S, Ridgway JM, Mahmood U, Su J, Shibuya TY, Crumley RL, Gu M, Armstrong WB, Chen Z: In vivo optical coherence tomography of the human larynx: normative and benign pathology in 82 patients. Laryngoscope 2005;115:1904–1911.

Wong BJ, Zhao Y, Yamaguchi M, Nassif N, Chen Z, de Boer JF: Imaging the internal structure of the rat cochlea using optical coherence tomography at 0.827 μm and 1.3 μm. Otolaryngol Head Neck Surg 2004;130:334–338.

Xu SA, Shepherd RK, Chen Y, Clark GM: Profound hearing loss in the cat following the single co-administration of kanamycin and ethacrynic acid. Hear Res 1993;70:205–215.

Yamakawa K: Über die pathologische Veränderung bei einem Ménière-Kranken. J Otolaryngol Soc Jpn 1938;4:2310–2312.

Yamasoba T, Kondo K: Supporting cell proliferation after hair cell injury in mature guinea pig cochlea in vivo. Cell Tissue Res 2006;325:23–31.

Downloaded by Keio University

Laboratory Investigation (2013) 93, 1001–1011
© 2013 USCAP, Inc All rights reserved 0023-6837/13

Morphological and functional changes in a new animal model of Ménière's disease

Naoya Egami[1], Akinobu Kakigi[1], Takashi Sakamoto[1], Taizo Takeda[2], Masamitsu Hyodo[2] and Tatsuya Yamasoba[1]

The purpose of this study was to clarify the underlying mechanism of vertiginous attacks in Ménière's disease (MD) while obtaining insight into water homeostasis in the inner ear using a new animal model. We conducted both histopathological and functional assessment of the vestibular system in the guinea-pig. In the first experiment, all animals were maintained 1 or 4 weeks after electrocauterization of the endolymphatic sac of the left ear and were given either saline or desmopressin (vasopressin type 2 receptor agonist). The temporal bones from both ears were harvested and the extent of endolymphatic hydrops was quantitatively assessed. In the second experiment, either 1 or 4 weeks after surgery, animals were assessed for balance disorders and nystagmus after the administration of saline or desmopressin. In the first experiment, the proportion of endolymphatic space in the cochlea and the saccule was significantly greater in ears that survived for 4 weeks after surgery and were given desmopressin compared with other groups. In the second experiment, all animals that underwent surgery and were given desmopressin showed spontaneous nystagmus and balance disorder, whereas all animals that had surgery but without desmopressin administration were asymptomatic. Our animal model induced severe endolymphatic hydrops in the cochlea and the saccule, and showed episodes of balance disorder along with spontaneous nystagmus. These findings suggest that administration of desmopressin can exacerbate endolymphatic hydrops because of acute V2 (vasopressin type 2 receptor)-mediated effects, and, when combined with endolymphathic sac dysfunction, can cause temporary vestibular abnormalities that are similar to the vertiginous attacks in patients with MD.

Laboratory Investigation (2013) **93,** 1001–1011; doi:10.1038/labinvest.2013.91; published online 22 July 2013

KEYWORDS: animal model; aquaporin; desmopressin; endolymphatic hydrops; Ménière's disease; vasopressin; vestibular disorder

Ménière's disease (MD) is a well-known inner ear disorder characterized by symptoms including recurring attacks of vertigo typically lasting for hours, fluctuating sensorineural hearing loss, and tinnitus. Since the milestone findings on the temporal bones of MD patients,[1,2] endolymphatic hydrops (EH) has been considered as the histopathological origin of MD, as characteristic morphological changes were reported to be produced by surgical obstruction of the endolymphatic sac (ES) in guinea-pig.[3] This observation indicates that malabsorption of endolymph in the ES is one of the possible mechanisms underlying the development of EH. This experimentally induced EH has been frequently used as an animal model to investigate the pathogenesis of inner ear disorders associated with EH. In terms of vestibular function, while canal dysfunction and/or spontaneous nystagmus have been occasionally observed in this animal model,[4,5] episodes of vertiginous attack or balance disorder have only rarely been observed.[6] In other words, this model is insufficient for fully representing the common symptoms of MD.

Water homeostasis of the inner ear is essential for maintaining the functions of hearing and balance. EH is considered to be the result of disruption of inner ear water homeostasis, which involves excessive production of endolymph and/or reduced absorption of endolymph. Until recently, however, the detailed mechanisms underlying the overaccumulation of endolymph were unclear. Since the discovery of aquaporin (AQP) water channels,[7] it has been proposed that precise regulation of water reabsorption largely depends on the regulation of AQP2 channels and that water permeability can change rapidly in response to vasopressin(VP).[8] Recently, it has come to light that this mechanism has a crucial role not only in the kidney but also in the inner ear. In addition, the following evidence has accumulated to suggest that VP is closely associated with the

[1]Department of Otolaryngology-Head and Neck Surgery, Faculty of Medicine, The University of Tokyo, Tokyo, Japan and [2]Department of Otolaryngology-Head and Neck Surgery, Kochi Medical School, Kochi, Japan
Correspondence: Dr A Kakigi, MD, Department of Otolaryngology, Faculty of Medicine, The University of Tokyo, 7-3-1 Hongo, Bunkyo-ku, Tokyo 113 8655, Japan.
E-mail: kakigi-tky@umin.ac.jp

Received 30 April 2013; revised 20 June 2013; accepted 22 June 2013

formation of EH: (1) plasma levels of arginine VP are higher in patients with MD and may depend on the phase that the patient is in,[9–11] (2) acute and chronic application of arginine VP produces EH in guinea-pigs and rats,[12–14] (3) V2 receptor mRNA is expressed in rat and human inner ear,[15–18] and (4) expression of V2 receptor mRNA in the rat inner ear is downregulated by VP application.[19] Such accumulated evidence has led to the assumption that production of endolymph is controlled by VP–AQP2 system.

In a previous study using an animal model of MD, Dunnebier *et al*[20] reported chronic ES dysfunction induced by destruction of the ES, and acute stress-induced endolymph production by aldosterone administration revealed severe degrees of hydrops in the cochlea.[20] In this investigation, we successfully developed a new clinically relevant animal model for MD, in which desmopressin (a VP type 2 receptor agonist) was administered after electrocauterization of the ES.

We evaluated both morphological and behavioral alterations of the vestibular system in this animal model to elucidate the role of VP in the pathogenesis of MD.

MATERIALS AND METHODS

This study was composed of two experiments. Experiment 1 was designed to investigate the influence of desmopressin on the development of EH morphologically. Experiment 2 was designed to investigate the role of desmopressin on changes in vestibular function. The animals used in Experiment 1 were albino outbred English short-haired guinea-pig (Hartley). In Experiment 2, pigmented English short-haired guinea-pig were used. Pigmented animals were selected for Experiment 2 to facilitate eye movement recording using an infrared-sensitive CCD camera.

These experiments were approved by Tokyo University Animal Care and Use Committee, and were conducted in accordance with The Animal Welfare Act and the guiding principles for animal care produced by the Ministry of Education, Culture, Sports, and Technology, Japan.

Experiment 1

Animals

A total of 24 guinea-pigs with a positive Preyer's reflex and weighing approximately 300 g were used in this experiment. All animals underwent electrocauterization of the ES of the left ear as reported previously.[21,22] The right ear was not treated surgically. The surgical procedures are described below (in the Surgical procedure for electrocauterization of the ES section). Animals were divided into two major groups. Twelve animals were allocated to survive for 1 week after electrocauterization of the ES and the other 12 for 4 weeks. In either group, six animals were given saline and the remaining six were treated with desmopressin systemically 1 h before euthanasia. In animals treated with desmopressin, 100 μg/kg (25 ml/kg) desmopressin acetate hydrate (desmopressin 4; Kyowa Hakko Kirin, Tokyo, Japan) was administered subcutaneously 1 h before euthanasia. In saline-treated animals, 25 ml/kg saline solution was administered subcutaneously 1 h before euthanasia. All animals were killed under deep anesthesia using ketamine and xylazine, and the temporal bones were collected from both sides. As shown in Figure 1a, 48 temporal bones harvested were classified into eight groups ($n=6$) according to the presence or absence of surgery, the survival duration, and type of treatment: (1) right temporal bones, 1-week survival after left ear electrocauterization, administered saline (1 W Control group (RIGHT)); (2) left temporal bones of the above-mentioned animals (1 W Surgery group (LEFT)); (3) right temporal bones, 1-week survival after left ear electrocauterization, administered desmopressin (1 W Desmopressin group (RIGHT)); (4) left temporal bones of the above-mentioned animals (1 W Combined group (LEFT)); (5) right temporal bones, 4-week survival after left ear electrocauterization, administered saline (4 W Control group (RIGHT)); (6) left temporal bones of the above-mentioned animals (4 W Surgery group (LEFT)); (7) right temporal bones, 4-week survival after left ear electrocauterization, administered desmopressin (4 W Desmopressin group (RIGHT)), and (8) left temporal bones of the above-mentioned animals (4 W Combined group (LEFT)).

Surgical procedure for Electrocauterization of the ES

All experimental animals were anesthetized by an intramuscular injection of ketamine (35 mg/kg) and xylazine (5 mg/kg). The animals received local anesthesia using xylocaine under sterile conditions. Subsequently, they were placed in a prone position with a head holder and underwent dorsal midline scalp incision. The left occipital bone was removed for visual exposure of the ES via an epidural occipital approach. Thereafter, the extraosseous portion of the sac was cauterized electrically with a bipolar electrocoagulator (Surgitron Model FFPF; Ellman International, Hewlett, NY, USA) so as not to injure the sigmoid sinus. The operation was performed using a Carl Zeiss operation microscope.

Quantitative Assessment of the Endolymphatic Space

Under deep anesthesia by an intraperitoneal injection of ketamine (35 mg/kg) and xylazine (5 mg/kg), all animals were perfused from the left ventricle with physiological saline solution, and then fixed with 10% formalin. The temporal bones were removed on both sides and postfixed in 10% formalin solution for 7 days. Subsequently, the specimens were decalcified in ethylenediamine tetraacetic acid for 14 days, and then dehydrated in a graded ethanol series before being embedded in paraffin. The prepared blocks were cut horizontally parallel to the axis of the modiolus into 6-μm sections. The sections were stained with hematoxylin and eosin for observation under a light microscope. We examined the degree of EH in the cochleae, vestibules, and semicircular canals using digital image measurement software, Micro Analyzer Ver. 1.1 (Nippon Poladigital, Tokyo, Japan).

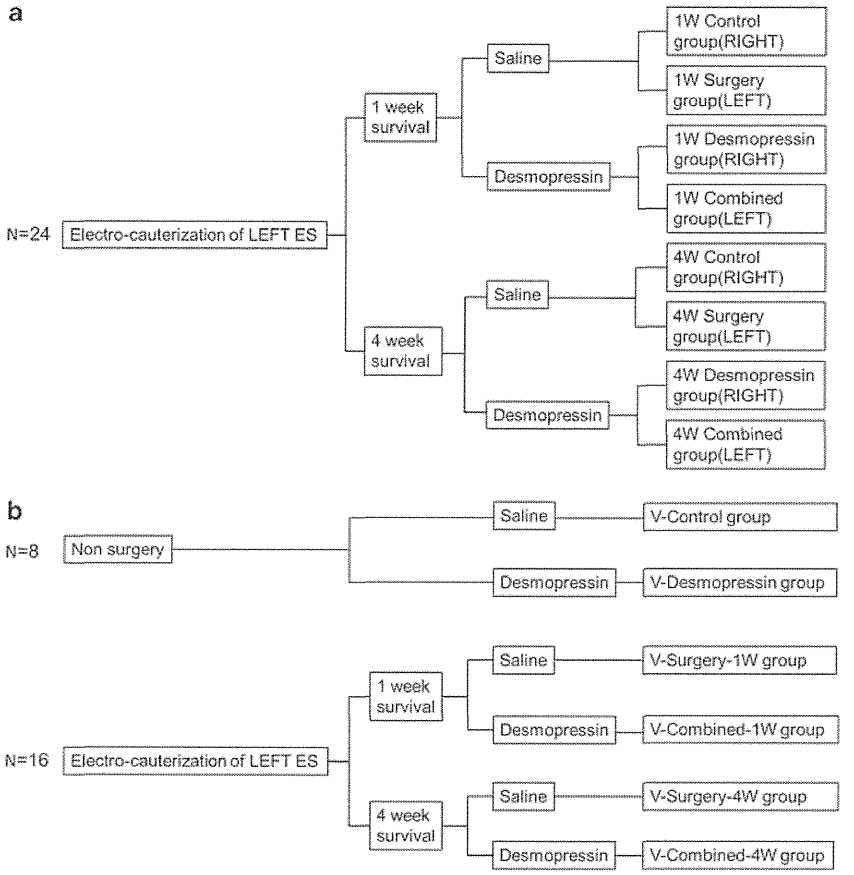

Figure 1 (**a**) Flow diagram of the experimental animals in Experiment 1. All animals underwent electrocauterization of the endolymphatic sac (ES) and duct on the left side and were randomly divided into two groups of either 1 or 4 weeks survival. The right ear of the saline administration group represents the 'Control group', and the left ear the 'Surgery group'. The right ear of the desmopressin administration group represents the 'Desmopressin group', and the left ear the 'Combined group'. (**b**) The study design of Experiment 2: (1) V-Control group; (2) *V-Desmopressin group*: animals without any surgical procedure, and with saline or desmopressin treatment 1 h before vestibular examination; (3) V-Surgery-1 W group; (4) *V-Combined-1 W group*: animals with electrocauterization of the ES after 1 week survival, and saline or desmopressin treatment 1 h before vestibular examination; (5) V-Surgery-4 W group; and (6) *V-Combined-4 W group*: animals with electrocauterization of the ES after 4 weeks survival, and saline or desmopressin treatment 1 h before vestibular examination.

To assess quantitatively the endolymphatic space variations across the cochlea turns, we measured the increase in the ratio of the cross-sectional area of the scala media (IR-S) in the basal, second, third, and apical turns, excluding the hook portion at the mid-modiolar sections. For this analysis, we used the following two parameters: (1) the cross-sectional area of the dilated scala media (Figure 2a, gray area), and (2) the cross-sectional area of the original scala media, enclosed by a straight line segment (Figure 2a, black area). This line segment represents the normal position of Reissner's membrane at the upper margin of the stria vascularis and its normal medial attachment at the spiral limbus. From these parameters, we calculated the increased ratios (%) of the cross-sectional area of the scala media (IR-S) of a total of four turns using the following formula:

Total IR-S (%) $= 100 \times (\sum(Ax - Bx)/xBx)$ (x: basal second, third, apical turn)

For the quantitative assessment of the spread of the endolymphatic space of the saccule, we measured the proportion of the area of the saccule (Figure 2b, gray area) relative to that of the vestibule (Figure 2b, black area) in the horizontal section including the stapes footplate. In the utricle, we also examined the proportion of the area of the utricle (Figure 2c, gray area) to that of the labyrinth (Figure 2c, black area) in the horizontal section including the crista of the lateral semicircular canal. For the semicircular canal, we examined the area of endolymph of the posterior semicircular canal (Figure 2d, gray area) relative to the area of bony posterior semicircular canal (Figure 2d, black area) in the horizontal section including the crista of the posterior semicircular canal.

Statistical Analyses

Differences in the degree of endolymph space by surgical procedure were evaluated for individual subjects by paired *t*-test. We compare the differences in the mean values among each group with Tukey's multiple comparison test. StatMate IV (ATMS, Tokyo, Japan) was used to conduct these analyses.

The data are presented as mean ± s.d., unless otherwise noted. A difference of $P<0.05$ was considered significant.

Experiment 2

Animals

A total of 24 pigmented guinea-pigs with a positive Preyer's reflex weighing approximately 300 g were used. Sixteen animals underwent electrocauterization of the ES in the left ear, and the remaining eight animals received no surgical procedure. The 16 animals that underwent surgery were divided into two groups, which were maintained for 1 week or 4 weeks before administration of saline or desmopressin. In either group, four animals were given saline and the remaining four animals were given desmopressin. Saline and desmopressin treatments were performed in the same manner as in Experiment 1. Animals that underwent surgery were assessed for evidence of a balance disorder and the presence of nystagmus for 1 h after they received a subcutaneous injection of 25 ml/kg saline solution, or 100 μg/kg (25 ml/kg) desmopressin acetate hydrate. Similarly in the eight surgery-free animals, vestibular examinations were undertaken for 1 h after administration of saline or desmopressin.

As shown in Figure 1b, experimental animals were classified into six groups ($n=4$) according to the presence or absence of surgery, the survival duration, and type of treatment: (1) *V-Control group*: surgery-free animals administered saline; (2) *V-Desmopressin group*: surgery-free animals administered desmopressin; (3) *V-Surgery-1 W group*: animals given saline 1 week after electrocauterization of the ES; (4) *V-Combined-1 W group*: animals given desmopressin 1 week after electrocauterization of the ES; (5) *V-Surgery-4 W group*: animals given saline 4 weeks after electrocauterization of the ES; and (6) *V-Combined-4 W group*: animals given desmopressin 4 weeks after electrocauterization of the ES.

Vestibular Examinations

We recorded spontaneous nystagmus with an eye movement recording system in a dark room for 1 h after administration of saline or desmopressin. The maximum slow-phase velocity was measured. The recording procedure has been described previously.[5] The dark iris can be detected using an infrared-

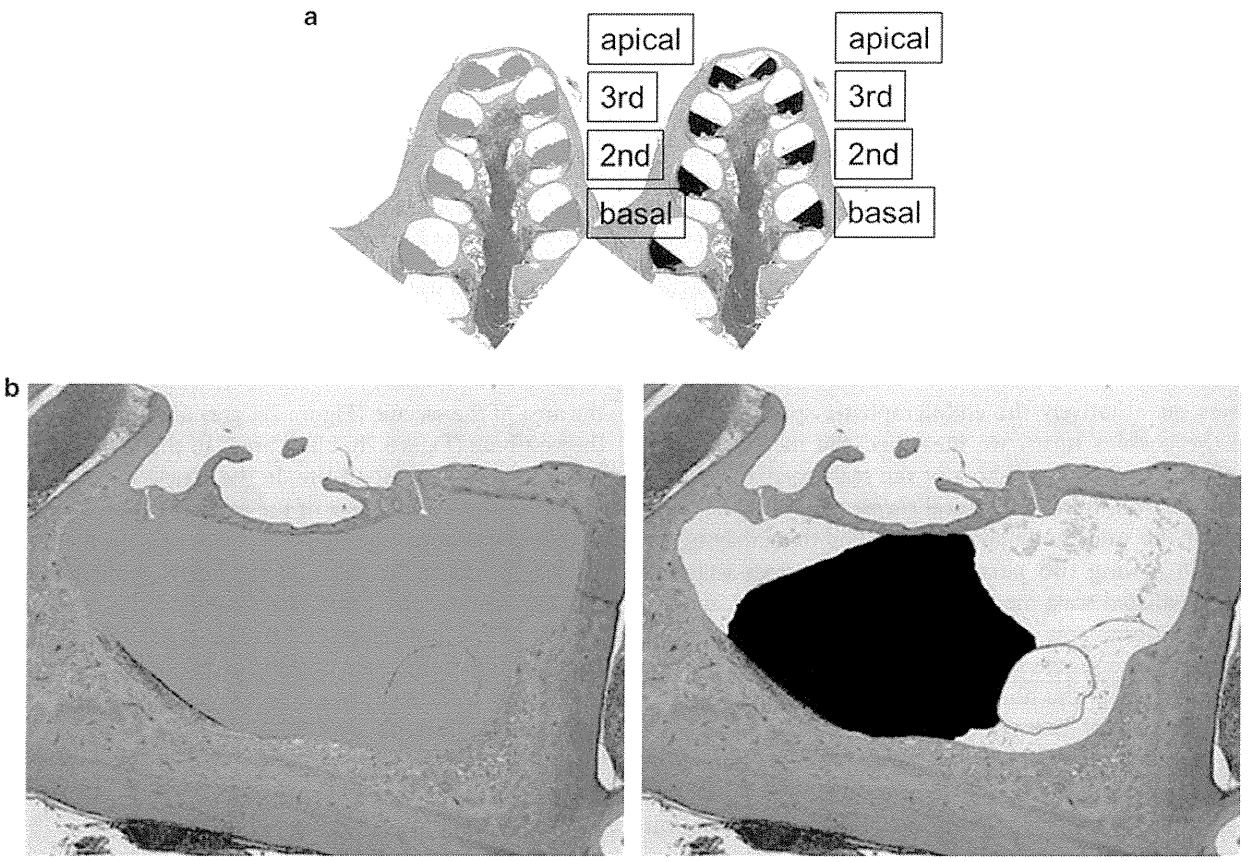

Figure 2 Parameters for the quantitative assessment of changes in the endolymphatic space. (**a**) The cross-sectional areas of the basal, 2nd, 3rd, and apical turns are indicated for the non-bulging scala media (gray, left) and the bulging scala media (black, right). (**b**) The vestibule (gray area, left) and the saccule (black area, right) in a horizontal section including the stapes footplate. (**c**) The labyrinth (gray area, left) and the utricle (black area, right) in a horizontal section including the crista of the lateral semicircular canal. (**d**) The bony posterior semicircular canal (gray area, left) and the endolymph of the posterior semicircular canal (black area, right) in a horizontal section including the crista of the posterior semicircular canal.

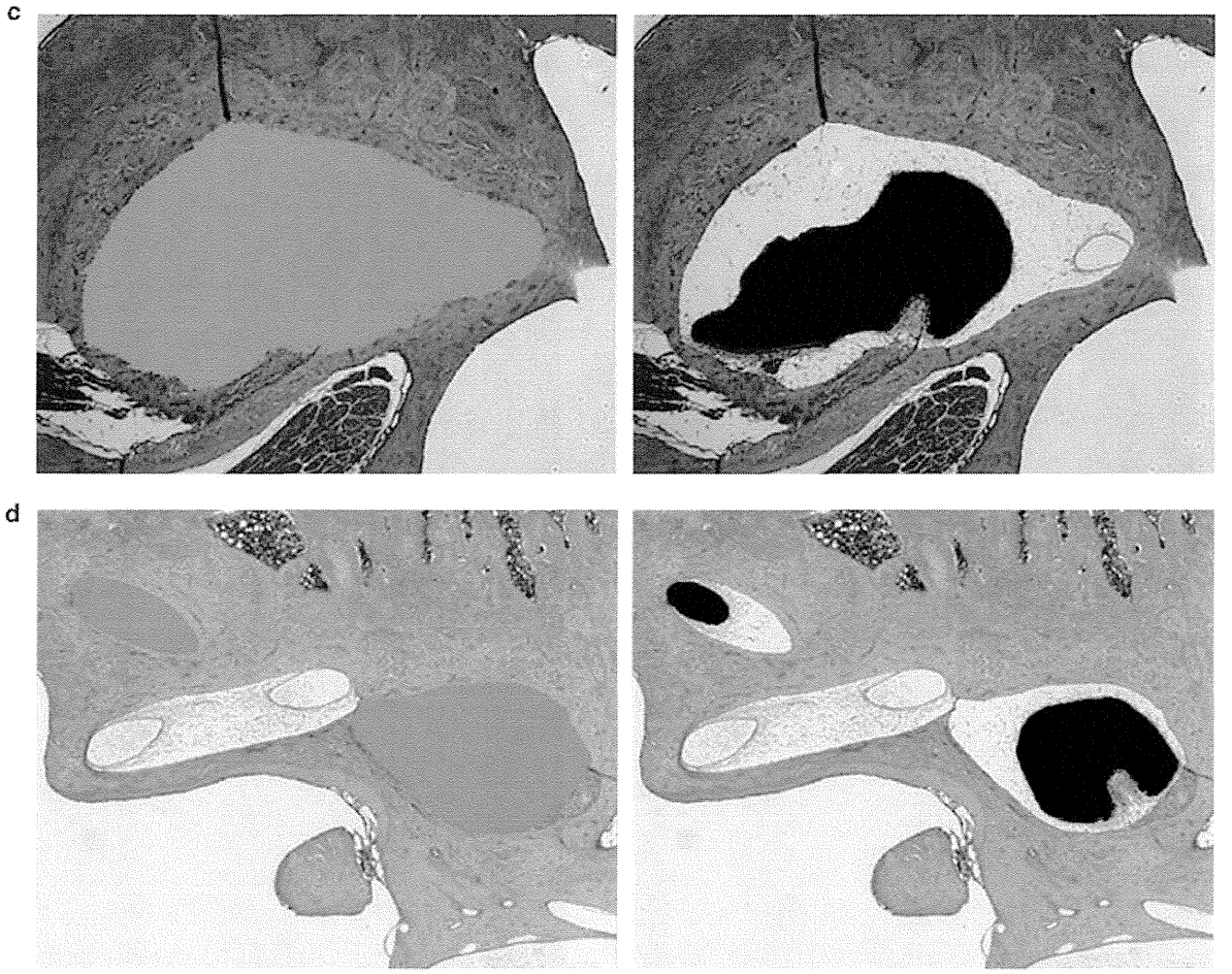

Figure 2 (Continued)

sensitive CCD camera to produce a binary image; the eye position and velocity are then calculated by a personal computer. We also monitored posture for 1 h after the administration of saline or desmopressin to determine the presence or absence of a balance disorder. Postural disturbances during a vestibular attack were videotaped.

RESULTS

Experiment 1

Figures 3 and 4 show representative pictures of the cochlea and the saccule in the four following groups: 4 W Control group, 4 W Surgery group, 4 W Desmopressin group, and 4 W Combined group. Reissner's membrane was almost straight in the 4 W Control group and 4 W Desmopressin group (Figures 3a and c), whereas it was moderately extended in the 4 W Surgery group (Figure 3b), and bulged into the scala vestibuli in the 4 W Combined group (Figure 3d). Saccular hydrops was not observed in the 4 W Control group or the 4 W Desmopressin group (Figures 4a and c), whereas the saccular space was moderately extended in the 4 W Surgery group (Figure 4b). In the 4 W Combined group, the saccular space was markedly extended and the saccular membrane was widely adhered to the stapes footplate (Figure 4d). There was no significant hydrops in the utricle or semicircular canal in any group, except that one animal in 4 W Combined group showed a slight expansion of the utricular space.

Figure 5 shows the results of quantitative analyses of the changes in the endolymphatic space in the cochlea, saccule, utricle, and the semicircular canal. In the cochlea, total IR-S (%) in the 1 W or 4 W Combined group showed a significantly greater ratio compared with the 1 W or 4 W Desmopressin group (paired *t*-test, $P<0.05$ and $P<0.01$, respectively; Figure 5a). In the 4 W Surgery group, the IR-S was significantly greater than that of the 4 W Control group (paired *t*-test, $P<0.05$; Figure 5a); however, the IR-S was not significantly different between 1 W Control group and 1 W Surgery group (paired *t*-test, $P>0.05$; Figure 5a). Total IR-S (%) in the 4 W Combined group was significantly greater when compared with the 1 W Surgery group, 1 W Combined group, and 4 W Surgery group (Tukey's multiple comparison test, $P<0.001$; Figure 5a). There were no significant

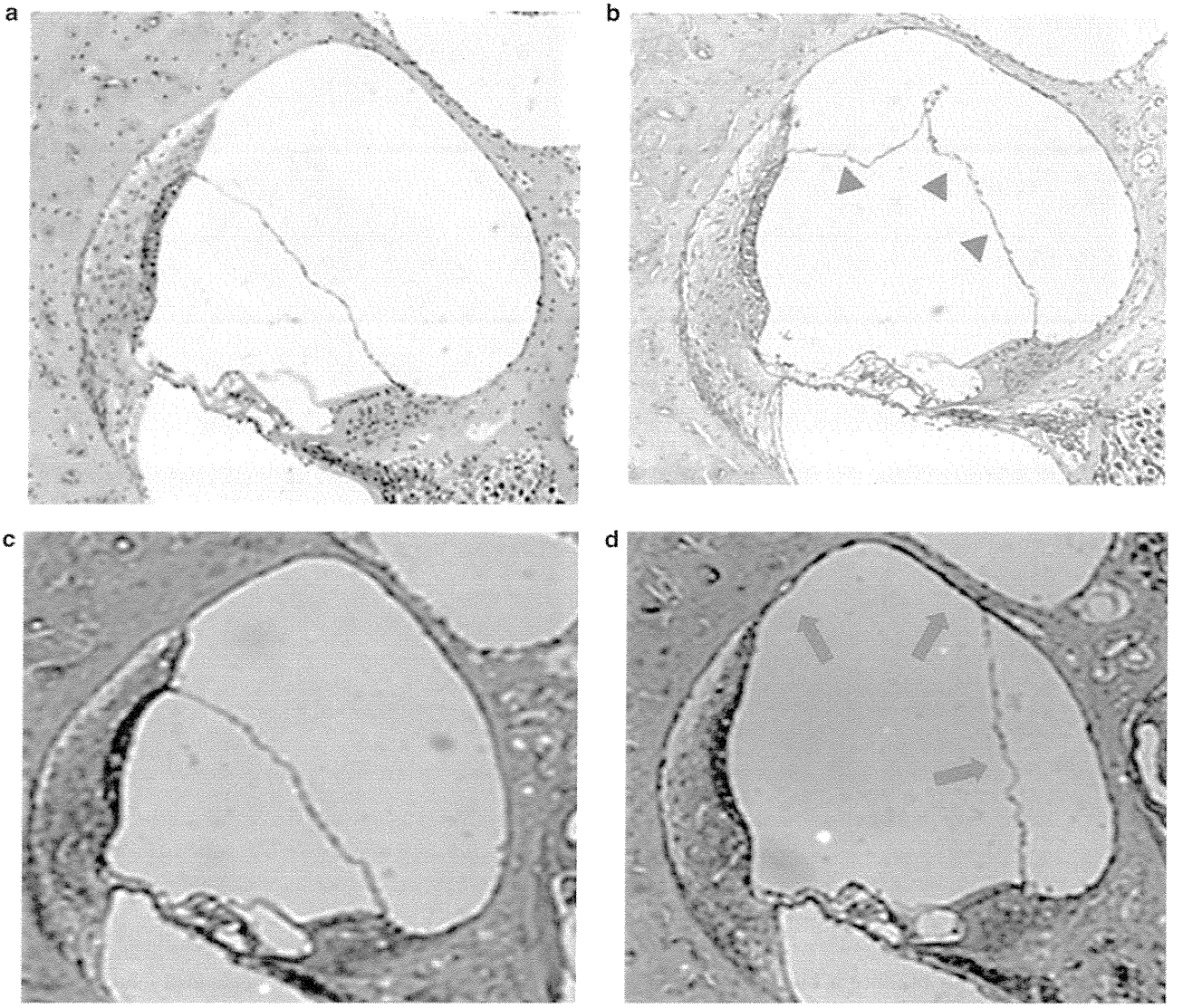

Figure 3 Representative pictures of the cochlea in the four ear groups maintained for 4 weeks: (**a**) saline-infused Control ear, (**b**) saline-infused Surgery ear, (**c**) desmopressin-infused Desmopressin ear, and (**d**) Combined ear. In the Surgery ear group, the scala media is distended and shows moderate hydrops (arrowhead). In the Combined ear, Reissner's membrane is bulging into the scala vestibule, which exhibits severe endolymphatic hydrops (arrow).

differences among 1 W and 4 W Control groups and 1 W and 4 W Desmopressin groups (Tukey's multiple comparison test, $P>0.05$; Figure 5a). Total IR-S (%) was significantly greater in the 4 W Combined group than in the 4 W Surgery group, and also in the 1 W Combined group than in the 1 W Surgery group (t-test, $P<0.05$; Figure 5a).

We also estimated the progression of cochlea EH in the Surgery and Combined groups. In the Surgery group, EH appeared to gradually develop over a time scale of weeks. The average growth rates of EH development in the Surgery group were estimated from the IR data in the 1 W or 4 W groups using the following formula: (IR-S (%) of the 1 W or 4 W Surgery groups − IR-S (%) of the 1 W or 4 W Control groups)/168 h (1 W) or 672 h (4 W). The average growth rates of EH development were 0.008%/h in the 1 W group and 0.025%/h in the 4 W group. In the Combined group, EH appeared to develop within 1 h of desmopressin administration. The average growth rates of EH development were estimated from the IR data using the following formula: IR-S (%) of the 1 W or 4 W Combined group − IR-S (%) of the 1 W or 4 W Surgical group. The average growth rates of EH development were $27.2-14.7\%=12.5\%$/h and $60.0-36.3\%=23.7\%$/h for the 1 W and 4 W groups, respectively.

The proportion of the saccular space was greater in the 1 W Combined group compared with the 1 W Desmopressin group (paired t-test, $P<0.05$; Figure 5b) and in the 4 W Combined group compared with the 4 W Desmopressin group (paired t-test, $P<0.001$; Figure 5b). In the 1 W and 4 W Surgery groups, the proportion of the saccular space was

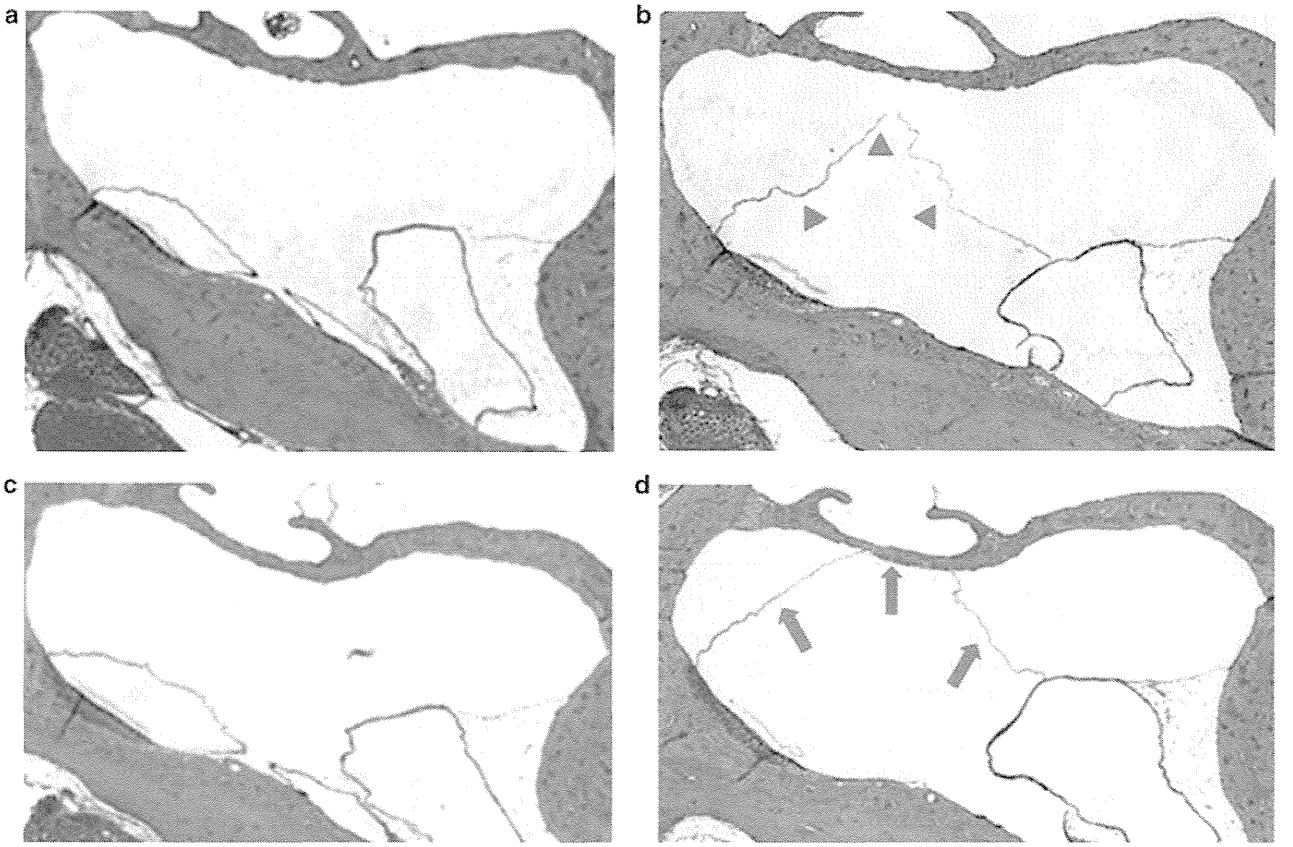

Figure 4 Representative pictures of the saccule in the four ear groups maintained for 4 weeks: (**a**) saline-infused Control ear, (**b**) saline-infused Surgery ear, (**c**) desmopressin-infused Desmopressin ear, and (**d**) Combined ear. In the Surgery ear group, moderate saccular hydrops can be seen (arrowhead). In the Combined ear group, severe saccular hydrops has extended to press against the stapes footplate (arrow).

significantly greater compared with the 1 W and 4 W Control groups (paired *t*-test, $P<0.05$ in both comparisons; Figure 5b). The proportion of the saccular space in the 4 W Combined group was significantly greater when compared with the 1 W Surgery group, 1 W Combined group, and 4 W Surgery group (Tukey's multiple comparison test, $P<0.001$; Figure 5b). There were no significant differences among the 1 W and 4 W Control groups and 1 W and 4 W Desmopressin groups (Tukey's multiple comparison test, $P>0.05$; Figure 5b). The proportion of the saccular space was significantly greater in the 4 W Combined group than in the 4 W Surgery group (*t*-test, $P<0.001$; Figure 5b), and also in the 1 W Combined group than in the 1 W Surgery group (*t*-test, $P<0.05$; Figure 5b).

We also estimated the progression of saccular hydrops in the Surgery and Combined groups. In the Surgery group, saccular hydrops appeared to develop over a time scale of weeks. The average growth rates of development of saccular hydrops was estimated from the proportion of saccular space remaining using the following formula for both the 1 W and 4 W groups: (proportion remaining (%) in the 1 W or 4 W Surgery group − proportion remaining (%) in the 1 W or 4 W Control group)/168 h (1 W) or 672 h (4 W). The average growth rates of development of saccular hydrops were 0.03%/h and 0.02%/h for the 1 W and 4 W groups, respectively. Comparing growth rates of development of saccular hydrops in the Surgery and Combined groups in the same manner yielded average speeds of $25.2 - 12.7\% = 12.5\%$/h for the 1 W group and $51.9 - 24.6\% = 27.3\%$/h for the combined group.

In the utricle, there were no significant differences among the four groups maintained for either 1 week or 4 weeks (Figure 5c). In both the semicircular canal ampulla and the duct, there were also no significant differences among the four groups maintained for either 1 week or 4 weeks (Figures 5d and e).

Experiment 2

All of animals in the V-Combined-1 W and V-Combined-4 W groups showed spontaneous nystagmus (Table 1 and Supplementary Movie 1 in Supplementary Material) and balance disorder (Supplementary Movie 2 in Supplementary Material). After the administration of desmopressin, one animal in the V-Desmopressin group demonstrated spontaneous nystagmus. No animals in the V-Control group, V-Surgery-1 W, and V-Surgery-4 W groups showed any nystagmus. Table 2 shows the maximum slow-phase velocity in the animals in the V-Combined-1 W and V-Combined -4 W

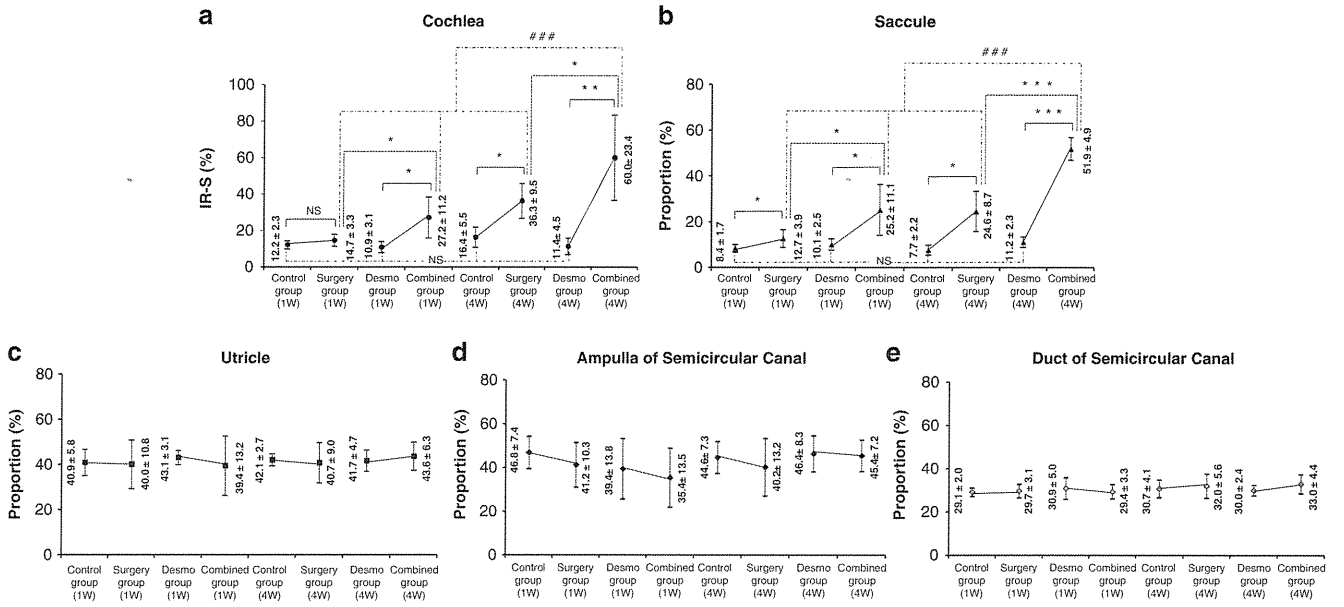

Figure 5 Result of quantitative analyses of the changes in endolymphatic space. (**a**) In the cochlea, total IR-S (%) in the Combined group maintained for 4 weeks showed a significant increase among four groups (paired *t*-test, $^{*}P<0.05$, $^{**}P<0.01$; *t*-test, $^{*}P<0.05$; Tukey's multiple comparison test, $^{\#\#\#}P<0.001$). (**b**) The proportion of the area of the saccule to that of the vestibule showed a significant increase in the Combined group maintained for 4 weeks (paired *t*-test, $^{*}P<0.05$, $^{***}P<0.001$; *t*-test, $^{*}P<0.05$, $^{***}P<0.001$; Tukey's multiple comparison test, $^{\#\#\#}P<0.001$). (**c**) The proportion of the area of the utricle to that of the vestibule showed no differences among either ear group or period of maintenance, 1 or 4 weeks. (**d**, **e**) In addition, the proportion of the area of the semicircular canal ampulla and duct to that of the vestibule showed no difference among either ear group or period of maintenance, 1 or 4 weeks.

groups, which presented spontaneous nystagmus. In cases 2, 6, and 7, the direction of nystagmus changed from the left to the right, indicating a change from irritative nystagmus to paralytic nystagmus. Typically, 10 min after the onset of the irritative nystagmus, the direction of nystagmus changed to the paralytic.

In cases 1, 5, and 8, only paralytic spontaneous nystagmus appeared (Supplementary Movie 1). In cases 3 and 4, only irritative spontaneous nystagmus appeared. The amplitude and direction of the maximum slow-phase velocity varied among the animals.

DISCUSSION

In this investigation, we successfully developed a new clinically relevant animal model for MD, in which desmopressin was administered after electrocauterization of the ES. In this animal model, distinct EH was evident in the cochlea and saccule, whereas there were no obvious changes in the utricle or semicircular canals. Temporal bone studies of patients with MD have revealed that EH is more frequently observed in the pars inferior than in the pars superior of the inner ear. It has been shown that severe EH is observed most frequently in the saccule, followed by the cochlea, utricle, and the semicircular canals.[23] Recent studies using magnetic resonance imaging have also confirmed these histopathologic findings.[24,25] In the Surgery group in Experiment 1, ears that underwent electrocauterization of the ES but without administration of desmopressin developed slight to moderate hydrops, indicating that prolonged ES dysfunction induced by electrocauterization may cause malabsorption of endolymph, and thus development of EH. This assumption is in line with following histopathologic findings related to the ES in patients with MD: poor development of the ES,[26,27] fibrotic changes of the ES, and a hypoplastic vestibular aqueduct.[28,29]

Experimentally induced EH, first proposed by Kimura and Schuknecht in 1965,[3] is well known as an animal model of MD. The EH of their model is thought to involve retention hydrops caused by the obliteration of the endolymphatic duct. This model animal is reported to have spontaneous nystagmus in the dark,[5,6,30] but not in the light.[31] In horizontal vestibular ocular reflex testing, vestibular ocular reflex gain was found to have decreased 1 week after the obliteration of ES.[5] These experimental results suggest that EH might contribute to vestibular dysfunction to some extent and that vestibular dysfunction might occur during the development and/or progression of EH. Episodes of temporary imbalance or vertigo, which are typical features of patients with MD, have not however been reported in animals that underwent obliteration of their ES. Therefore, such animals with EH due only to the retention of endolymph are not considered suitable as an animal model of MD.

Considering these issues, we speculated that the lack of temporary vestibular episodes in the classical MD animal model might be related to growth rates of formation of EH, not the degree of EH. That is, the development

of EH caused by malabsorption in the ES is too slow to produce a vertiginous attack. Indeed, animals that survived for 4 weeks after electrocauterization of the left ES (4 W Surgery group) developed severe EH in the cochlea and the saccule, but showed no distinct vestibular disorders. Therefore, we modified the classical animal model with the additional administration of desmopressin to accelerate the development of EH.

As expected, animals given desmopressin 1 or 4 weeks after the electrocauterization of the ES showed both spontaneous nystagmus and balance disorders (V-Combined-1 W group and V-Combined-4 W group). Most of the V-Combined group animal showed desmopressin-induced vestibular disorders about 1 h, which agrees with the time course of desmopressin-induced intrastrial space enlargement.[32] Morphological changes indicated that animals that survived for 4 weeks after the electrocauterization of the left ES combined with administration of desmopressin (4 W Combined group) had severe EH in the cochlea and the saccule, and that the degree of EH was extremely high compared with animals that survived for only 1 week after electrocauterization of the left ES and the administration of desmopressin (1 W Combined group) even though both groups demonstrated episodes of vestibular dysfunction. The degree of EH and the saccular hydrops in the 1 W and 4 W combined groups was extremely high compared with animals that survived for 1 or 4 weeks after the electrocauterization of the left ES alone (1 W and 4 W Surgery group) (Figure 5a and b). Thus, the disorders of vestibular function could not be rationalized on the basis of the degree of EH. With the dynamic changes of EH in mind, however, another theory could be proposed. In the 1 W and 4 W Surgery groups, EH is thought to develop gradually over 1 and 4 weeks. On the other hand, EH in animals administered desmopressin is thought to develop as rapidly as within 1 h. Analysis of the average growth rates of EH development, estimated from the IR and proportion of saccular space, indicates that animals in the Combined groups had very high growth rates of EH development both in the cochlea and in the saccule, regardless of the survival time between surgery and the measurement. Taking these results into consideration, the desmopressin-induced vestibular disorders in animals in the V-Combined-1 W group are readily understandable.

Generally, EH is well known to exist in cases with a clinical diagnosis of Meniere's syndrome. Conversely, nearly one-third of the cases of idiopathic hydrops show no association with the classic symptoms of Meniere's syndrome.[33] In addition, previous histopathological examinations have revealed that the contralateral ears of patients with unilateral Meniere's disease showed asymptomatic saccular hydrops in around 30% of patients.[34,35] Recently, Kato *et al*[36] reported that there was no significant association between the degree of EH and caloric responses, using MRI. Previous studies have suggested that not only static morphological hydrops but also dynamic changes of hydrops may be responsible for the symptoms of MD, and further support the validity of our new animal model for MD.

Table 1 Presence or absence of spontaneous nystagmus in experimental animals

	Spontaneous nystagmus	
	Positive (%)	*Negative* (%)
V-Control group	0	100
V-Desmopressin group	25	75
V-Surgery-1 W group	0	100
V-Surgery-4 W group	0	100
V-Combined-1 W group	100	0
V-Combined-4 W group	100	0

Table 2 Maximum slow-phase velocity in animals with spontaneous nystagmus

1 Week after Surgery	*MSPV*
Animal 1	−3.71
Animal 2	3.99 → −1.09
Animal 3	14.7
Animal 4	2.41
4 Weeks after surgery	
Animal 5	−5.08
Animal 6	6.51 → −6.8
Animal 7	5.59 → −2.47
Animal 8	−3.66

Abbreviation: MSPV, maximum slow-phase velocity (°/s).
Positive and negative values are nystagmus toward surgical (left) and non-surgical (right) ears, respectively. In animals 2, 6, and 7, spontaneous nystagmus switch from irritative to paralytic.

Endolymph flow measurements show that endolymph does not flow along the cochlea and it is generally agreed that most of the potassium in endolymph is recycled between perilymph and endolymph.[37,38] When the ES is in a normal state, the secretion and absorption of endolymph are well balanced. Previous molecular biological studies revealed that AQP2 mRNA expression in the cochlea as well as in the ES was upregulated by systemic application of VP.[39] Morphologically, the endolymphatic space was found to increase in response to systemic application of VP.[13] Clinically, Takeda *et al*[9] demonstrated evidence of elevated serum arginine VP levels in patients with MD. Hornibrool *et al*[40] reported that there have not been abnormal plasma levels of arginine VP in patients of MD. The reasons for these controversial results might have been that because platelets

present in plasma cause overestimation of plasma arginine VP and partly to avoid degradation of AVP activity resulting from its short half-life,[41–43] it might be one of the most important reasons for the great differences in basal arginine VP concentrations observed in different laboratories. These previous experimental findings indicate that the water homeostasis of the inner ear fluid is partly regulated via the VP–AQP2 system. In this study, desmopressin (V2 agonist) was used to examine the V2 effect of VP, not the *vasopressin* type 1 (V1) effect, because the V1 receptor, although limited to mRNA, is also expressed in the inner ear.[44,45]

On the basis of previous and present investigations, and given that patients with EH alone do not suffer from vertigo, we assume that the pathogenesis of vertiginous attacks is as follows: activation of the VP–AQP2 system by the V2 effect may yield overproduction of endolymph, with an increase in the influx of water from the perilymph into the endolymph, which causes sudden changes in endolymphatic pressure. We speculate that under chronic endolymphatic dysfunction, it may reduce absorption of endolymph and chemical mechanisms can concomitantly cause Meniere's symptoms. Chemical factors include hydrostatic pressure alterations, it changes membrane permeability, causing inappropriate ion across the membrane barrier so as to incite sensory dendrites and lead to cochlear and vestibular symptoms. In our experiment, we can see a remarkable histopathological change in the cochlea and saccule, not in the utricle and semicircular canals. There remains some discussion about whether an endolymph–perilymph pressure gradient may cause these morphological variations. Previous studies have shown that AQP2 protein and/or mRNA are expressed in the inner ear of rats.[19,39,46] Furthermore, the V2 receptor and/or its mRNA are found in the cochlea.[16,18] These previous studies suggest that water homeostasis in the inner ear is partly regulated via the VP–AQP2 system. If AQP2 protein and/or mRNA was to be overexpressed in the stria vascularis or vestibular dark cells, the VP–AQP2 system may promote overproduction of endolymph. Therefore, the difference in AQP2 expression in the stria vascularis and the dark cells may cause morphological variations. Further study is needed to determine the mechanism of the VP–AQP2 system in the inner ear using this animal model to understand the relationship between VP and MD.

Supplementary Information accompanies the paper on the Laboratory Investigation website (http://www.laboratoryinvestigation.org)

DISCLOSURE/CONFLICT OF INTEREST
The authors declare no conflict of interest.

1. Yamakawa K. Uber die pathologische Veranderung bei einem Meniere-Kranken. J Otorhinolaryngol Soc Jpn 1938;44:2310–2312.
2. Hallpike CS, Cairns H. Observations on the pathology of Meniere's syndrome. J Laryngol Otol 1938;53:625–655.
3. Kimura RS, Schuknecht H. Membranous hydrops in the inner ear of the guinea pig after the obliteration of the endolymphatic sac. Pract Otorhinolaryngol 1965;27:343–354.
4. Manni JJ, Kuijpers W, Huygen PLM, *et al.* Cochlear and vestibular functions of the rat after obliteration of the endolymphatic sac. Hear Res 1988;36:139–152.
5. Kakigi A, Taguchi T, Takeda T, *et al.* Time course of vestibular function changes of experimental endolymphatic hydrops in guinea pigs. ORL 2010;71(Suppl 1):19–25.
6. Andrews JC, Honrubia V. Vestibular function in experimental endolymphatic hydrops. Laryngoscope 1988;98:479–485.
7. Agre P, Sasaki S, Chrispeels MJ. Aquaporins: a family of water channel proteins. Am J Physiol Renal Physiol 1993;265:F461.
8. Nielsen S, Fronkiare J, Marples D, *et al.* Aquaporins in the kidney: from molecules to medicine. Physiol Rev 2002;82:205–244.
9. Takeda T, Kakigi A, Saito H. Antidiuretic hormone (ADH) and endolymphatic hydrops. Acta Otolaryngol Stockh 1995;519: 219–222.
10. Aoki M, Ando K, Kuze B, *et al.* The association of antidiuretic hormone levels with an attack of Ménière's disease. Clin Otolaryngol 2005;30:521–525.
11. Takeda T, Takeda S, Kakigi A, *et al.* Hormonal aspects of Ménière's disease on the basis of clinical and experimental studies. ORL 2009;71(Suppl 1):1–9.
12. Kumagami H, Lowewenheim H, Beitz E, *et al.* The effect of anti-diuretic hormone on the endolymphatic sac of the inner ear. Pflugers Arch 1998;436:970–975.
13. Takeda T, Takeda S, Kitano H, *et al.* Endolymphatic hydrops induced by chronic administration of vasopressin. Hear Res 2000; 140:1–6.
14. Kitano H, Takeda T, Takeda S, *et al.* Endolymphatic hydrops by administration of vasopressin in the rat. Acta Histochem Cytochem 2001;34: 229–233.
15. Kitano H, Takeda T, Suzuki M, *et al.* Vasopressin and oxytocin receptor mRNAs are expressed in the rat inner ear. NeuroReport 1997;8: 2289–2292.
16. Taguchi D, Takeda T, Kakigi A, *et al.* Expressions of aquaporin-2, vasopressin type 2 receptor, transient receptor potential channel vanilloid (TRPV)1, and TRPV4 in the human endolymphatic sac. Laryngoscope 2007;117:695–698.
17. Nishimura M, Kakigi A, Takeda T, *et al.* Expression of aquaporins, vasopressin type 2 receptor, and $Na^+( )K^+( )^-$ cotransporters in the rat endolymphatic sac. Acta Otolaryngol 2009;129:812–818.
18. Nishioka R, Takeda T, Kakigi A, *et al.* Expression of aquaporins and vasopressin type 2 receptor in the stria vascularis of the cochlea. Hear Res 2010;260:11–19.
19. Kitano H, Suzuki M, Kitanishi T, *et al.* Regulation of inner ear fluid in the rat by vasopressin. NeuroReport 1999;10:1205–1207.
20. Dunnebier EA, Segenhout JM, Wit HP, *et al.* Two-phase endolymphatic hydrops: a new dynamic guinea pig model. Acta Otolaryngol 1997;117:13–19.
21. Lee KS, Kimura RS. Ischemia of the endolymphatic sac. Acta Otolaryngol (Stockh) 1992;112:658–666.
22. Takeda T, Kakigi A, Saito H. Epidural electrocauterization of endolymphatic sac. Equilibrium Res 1993;9(Suppl):139–143.
23. Okuno T, Sando I. Localization, frequency and severity of endolymphatic hydrops and the payhology of the labyrinthine membrane in Meniere's disease. Ann Otol Rhinol Laryngol 1987;96:438–445.
24. Nakashima T, Naganawa S, Sugiura M, *et al.* Visualization of endolymphatic hydrops in patients with Meniere's disease. Laryngoscope 2007;117:415–420.
25. Fiorino F, Pizzini FB, Beltramello A, *et al.* Progression of endolymphatic hydrops in Ménière's disease as evaluated by magnetic resonance imaging. Otol Neurotol 2011;32:1152–1157.
26. Shambaugh GE, Clemis JD, Arenberg IK. Endolymphatic duct and sac in Meniere's disease. 1. Surgical and histopathologic observations. Arch Otolaryngol, 89:816–825.
27. Takeda T, Sawada S, Kakigi A, *et al.* Computed radiographic measurement of the dimensions of the vestibular aqueduct in Meniere's disease. Acta Otolaryngol (Stockh) 1997;528(Suppl): 80–84.
28. Sando I, Ikeda M. The vestibular aqueduct in patients with Meniere's disease. Acta Otolaryngol (Stockh) 1984;97:558–570.